AD-781 479

SURVEY OF CURRENT FRACTURE MECHANICS STUDIES AT AMMRC

Joseph I. Bluhm

Army Materials and Mechanics Research Center
Watertown, Massachusetts

July 1972

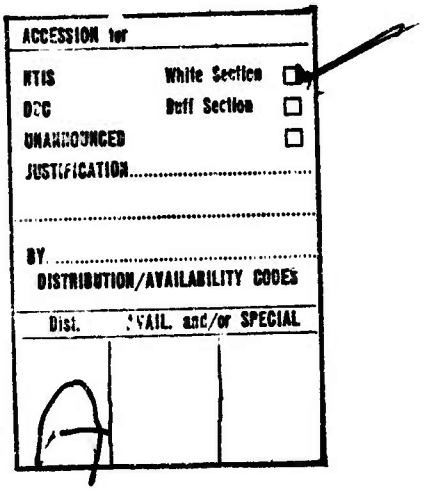

The findings in this report are not to be construed as an official Department of the Army position, unless so designated by other authorized documents.

Mention of any trade names or manufacturers in this report shall not be construed as advertising nor as an official indorsement or approval of such products or companies by the United States Government.

DISPOSITION INSTRUCTIONS

Destroy this report when it is no longer needed.
Do not return it to the originator.

AD781 479

DOCUMENT CONTROL DATA - R & D

(Security classification of title, body of abstract and indexing annotation must be entered when the overall report is classified)

1. ORIGINATING ACTIVITY (Corporate author)
Army Materials and Mechanics Research Center
Watertown, Massachusetts 02172

2a. REPORT SECURITY CLASSIFICATION
Unclassified

2b. GROUP

3. REPORT TITLE

SURVEY OF CURRENT FRACTURE MECHANICS STUDIES AT AMMRC

4. DESCRIPTIVE NOTES (Type of report and inclusive dates)

5. AUTHOR(S) (First name, middle initial, last name)
Joseph T. Bluhm

6. REPORT DATE
July 1972

7a. TOTAL NO. OF PAGES
76

7b. NO. OF REFS
21

8a. CONTRACT OR GRANT NO.

b. PROJECT NO. D/A 1T062105A331

c. AMCMS Code Number 502E.11.297-X090100

d.

9a. ORIGINATOR'S REPORT NUMBER(S)
AMMRC MS 72-7

9b. OTHER REPORT NO(S) (Any other numbers that may be assigned this report)

10. DISTRIBUTION STATEMENT

Approved for public release; distribution unlimited.

11. SUPPLEMENTARY NOTES

12. SPONSORING MILITARY ACTIVITY
U. S. Army Materiel Command
Washington, D. C. 20315

13. ABSTRACT

The fracture and fatigue studies at AMMRC encompass both experimental and analytical thrusts. This presentation will cover a few representative activities.

The status of test program on fracture behavior of unidirectionally reinforced composites using double cantilevered type specimens will be reported. Material systems include "S" glass/epoxy and graphite/epoxy. Limited fracture toughness data is available. Additionally, some effort has been initiated on cross ply specimens.

Fatigue studies at AMMRC in metals reflect a continuing interest in both initiation and propagation aspects. A technique has been developed for detection of crack initiation using an automated photographic process for recording, periodically, potential initiation sites. The observations are discussed in conjunction with damage criteria. Crack propagation studies have focussed in developing a "law" which accounts for the extremes of propagation rates at threshold levels of stress intensity and at the higher levels associated with unstable growth. Additionally, crack propagation experiments are described which are aimed at exploring the transient effects on crack propagation of sudden changes in stress intensity levels.

Supplementing these experimental studies are extensive analytical efforts directed toward defining the stress states in anisotropic material when used in lap and/or mechanical joint configurations. Additionally, extensive effort by one team of investigators has been devoted to analytical techniques for crack analysis. These techniques have been applied to a wide variety of geometric configurations and to a range of material types including anisotropic. This effort will be described briefly. (Author)

DD FORM 1 NOV 68 1473 REPLACES DD FORM 1473, 1 JAN 64, WHICH IS OBSOLETE FOR ARMY USE.

14 KEY WORDS	LINK A		LINK B		LINK C	
	ROLE	WT	ROLE	WT	ROLE	WT
Fracture (materials) Fatigue (materials) Mechanics						

AMMRC MS 72-7

SURVEY OF CURRENT FRACTURE MECHANICS STUDIES AT AMMRC

Monograph by
JOSEPH I. BLUHM

July 1972

D/A Project 1T062105A331
AMCMS Code 502E.11.297-XO90100
Composite Materials Research for Army Materiel

MECHANICS RESEARCH LABORATORY
ARMY MATERIALS AND MECHANICS RESEARCH CENTER
Watertown, Massachusetts 02172

Presented at Symposium on Fracture and Fatigue at George Washington University, Washington, D.C. on May 3, 1972.

LIST OF ILLUSTRATIONS

CONTENTS

I. INTRODUCTION

Within the Army Materiel Command, AMMRC, the Army Materials and Mechanics Research Center at Watertown, Mass., has the responsibility for research in structural materials and mechanics.

The scope of that mechanics responsibility is portrayed in Figure 1. I shall describe the effort of only two of the areas shown - namely fracture and fatigue.

In the fracture regime I will discuss some of our experimental studies in the mechanical behavior of layered fibrous composites - both unidirectional as well as angle ply; I will mention some of the unique characteristics of these angle ply composites in producing stress concentrations near free edges even in the absence of gross geometric notches, and then I'll cover our purely analytical studies in fracture mechanics, particularly as oriented toward anisotropic materials. Finally I will conclude the fracture discussion with a fleeting reference to some interests in dynamic fracture.

In the area of fatigue I will describe briefly a crack initiation study and a study examining the transient growth rate of cracks when subjected to a step change in the applied stress intensity factor.

I wish to indicate at the outset that my role as speaker is as a reporter of other people's work. I will attempt to identify and acknowledge these contributors as I proceed.

II. FRACTURE

Slepetz of our staff is carrying out an in-depth investigation of the fracture behavior of unidirectional[1] and cross ply filamentary layered composites. Figures 2 and 3 show superficially the nature of his investigation. Using specimens of the compact tension type shown, he has obtained, at least for unidirectionally reinforced composites, load deformation curves of the type shown. These characteristically showed a series of successive load drops corresponding to "pop-ins" early in the loading sequence, but these eventually damped out and disappeared as loading and crack extension proceeded. With these load deformation curves and experimentally determined compliance curves as shown, the end result, the fracture toughness, was easily obtained using the relation

$$G_c = (F^2/2t)(dc/da) \qquad (1)$$

Representative curves for two material systems are shown. The early rise in the G_c vs a curves is associated with the pop-in behavior; the later sharp rise occurs when the crack approaches the far end of the specimen.

Figure 4 shows the more detailed compliance data obtained for the unidirectionally reinforced S-glass/epoxy specimen. This shows compliance C plotted against dimensionless crack length a/w. The solid line represents the equation shown. This equation is based upon a simple strength of materials analysis with coefficient determined to match the experimental points. The analytical expression was then used to determine dc/da for use in Equation 1. Figure 5 shows the bulk of fracture toughness data obtained for this type specimen. Note as in Figure 2 the early pop-in region, followed by the steady state stage and the ultimate sharp rise. Figure 6 shows the corresponding toughness data for unidirectional reinforced specimens with fibers at various other orientations. Again the same trends are noted. However, it is noted

that no attempt was made in analyzing these latter specimens to separate effects of the crack opening stress intensity factor K_I from the in-plane stress intensity factor, K_{II}.

The next figure (Figure 7) shows some of the effects of cross ply reinforcement, i.e., where adjacent layers have their respective fibers in different directions. It has been earlier noted that for unidirectional composites the cracks always form parallel to the fibers; in cross ply cases the cracks still tend to follow the fiber direction for the particular layer in which the crack exists. The interaction of the crack systems in adjacent layers leads to excessive interlaminar shear stresses and ultimate debonding or delamination. Furthermore, as the "crack" progresses by this mechanism, we are not exactly sure of the appropriate way of defining a fracture toughness quantity.

To get a better base line for understanding the behavior of these fibrous composites we have undertaken an examination of the deformation and strain field at the crack tip region. Figure 8 shows some preliminary results of deformation fields in a unidirectionally reinforced specimen using moiré interference techniques. These studies were carried out by Slepetz and Prof. Fu Pen Chiang of State University of New York at Stonybrook College[2].

The upper row of interference patterns was made using a 300 line/inch grating and white diffuse light. The second and third rows were taken using an optical multiplication system which provided 600 and 1200 lines/inch respectively. The columns correspond to crossed grids, horizontal grids and vertical grids, respectively. These grid arrangements provide all the deformation components. Analysis of these results has not been completed yet.

These materials characterization studies are being coordinated with large scale panel tests incorporating stiffeners in order to validate the

applicability of the toughness measurement and to substantiate recently completed analysis by Lakshmikantham which will be discussed later. Specifically, a test program is underway to observe the fracture and fracture arrest characteristics of stiffened flat panels. Material systems being examined in the panel study include fiber glass/epoxy, graphite/epoxy, and boron/aluminum. Instrumentation will be predominantly strain gage and moiré grids.

Another important trait of angle ply layered composites is the edge effects they display; significant stress concentrations are evidenced even in "simple" unnotched tension strips. Oplinger et al of our staff have been investigating this both experimentally and analytically[3][4]. Figure 9 shows the trend of the in-plane deformation field as well as the interlaminar shear stress distribution. Note the non-symmetry of the deformations. This is caused by virtue of the fact that the filaments in each layer tend to reorient themselves, under load, into the direction of the tension load. In doing this there is a scissoring action between adjacent crossed layers and this sets up the high interlaminar shear stresses shown. Figure 10 shows some experimental results again using moiré gratings to determine the deformation fields. The upper views show the grating direction and the resulting in-plane deformation pattern substantiating the predicted trend shown in Figure 9. The lower views show the moiré fringe pattern looking in on the edge. The quality of the fringe pattern is not good; on the other hand, it is pointed out that this specimen is only .085" thick, and techniques for applying gratings under such circumstances are not well developed. However, again the fringe pattern is consistent with the prediction and provides substantiation of the presence of the interlaminar shear stresses. Figure 11 shows the variation of the fringe pattern with applied load for these same specimens.

The effect of stacking sequence is illustrated in Figure 12. This shows the interlaminar shear distribution in a 24-layered filamentary composite for two stacking sequences. The left curve is for a clustered sequence, i.e., twelve (12) in one orientation and then twelve in the crossed orientation. This leads to a rather significant stress concentration factor of approximately 2.6 at the edge. On the other hand, if the 24 layers are stacked in alternating orientations, i.e. $+\theta$, $-\theta$, $+\theta$, ..., then the peak stresses are significantly reduced and the stress concentration factor is approximately 1.27.

Oplinger has also treated[3] the problem of edge effects as influenced by the structure of reinforcing filaments such as graphite or glass yarns. His results, shown schematically in Figure 13, reveal, for example, that yarn reinforcement gives rise to more pronounced deformation gradients and correspondingly to much higher interlaminar shear stresses than with large filament reinforcements.

Figure 14 summarizes the range of experiments anticipated in connection with these edge effect studies. Both clustered and alternating stacking sequences will be investigated, and the range of ply angles will span from $\pm 10^{\circ}$ to $\pm 45^{\circ}$. Several material systems will be explored, i.e., boron/epoxy, graphite/epoxy, and boron/aluminum. To date the concentration of effort has been for the boron/epoxy system with a clustered stacking sequence at $\pm 20^{\circ}$.

Oplinger and Gandhi are also engaged in analytical studies of joint design. Two generic configurations are being examined, the adhesively bonded lap joint and the mechanical (pinned) joint. As suggested in Figure 15, the focus of effort here is on layered composite constituents. The layered plate with circular hole is being examined to provide input for the detailed solution of the pin joint problem. As a preliminary to more general lap joint problems, Gandhi[5] has completed and programmed the plane

strain analysis of a lap joint with isotropic constituents and zero thickness bond. The configuration and results for both the bond layer shear and tensile stresses are shown in Figure 16. The singularity of the corners, neglected in this first approach, is currently being introduced into the solution. The pin joint problem has been carried out by Oplinger and Gandhi[6], and initial results are shown in Figure 17. The solution here is for a "rigid" pin in an infinite, homogeneous but anisotropic plate with perfect fit. A computer program has been completed. The stress levels are given for an applied pin load of 100 lbs. per inch. The stress distribution is given for the hole boundary, i.e., at $\gamma = a$, and also for a circular path at $\gamma = 1.5a$. To account for the presence of the laminae, a separate analysis is underway as implied above treating the physical problem shown in the upper left of Figure 15. Here an infinite layered plate with a hole subject to tension is being analyzed. The thickness variations associated with the change in lamina modulus with each layer are being treated. Results of this solution will then be integrated with the rigid pin solution to obtain the total solution. The results will also be extended to account for finite width specimens.

One of the principal areas of potentially fruitful exploitation of fracture mechanics is in the prediction of residual strength and crack arrest properties of critical structural components of military vehicles (aircraft, etc.) where those components have been damaged in a combat situation. Figure 18 suggests schematically one technique for arrest. We are initially undertaking a study of the structural mechanics effects from damage due to penetration by fragments and/or projectiles. Structural damage due to blast loadings is considered for study at a later date.

Rich[7] of our staff, after surveying the current state-of-the-art of battle damage analysis, has defined three approaches to projectile damage:

1) Empirical approach based upon residual strength tests of projectile damaged components; 2) Statistical approach based upon reliability studies of residual strength tests; and 3) Analytical approach based upon stress computations of representative damage configurations plus appropriate failure criteria. In the first two approaches a measure of damage is required to correlate results; one such possibility is shown as an "effective" damage crack length in Figure 19. To evaluate all three approaches, we are conducting residual strength tests on: a) controlled, simulated battle damage components; and b) actual ballistically damaged components as suggested in Figure 20. The eventual product of these studies will be residual strength curves for the best measurement of battle damage. These curves should aid both the designer of future equipment in selecting designs of reduced vulnerability and the field commander in assessing the operational limitations on current equipment.

With the exception of the immediately preceding discussion of residual strength, I have been focusing attention on heterogeneous materials and their fracture behavior. Since analysis, taking this heterogeneity into account, in any depth is extremely difficult and cumbersome, considerable effort has been devoted by the staff here at AMMRC to an alternative of considering the problems of homogeneous but anisotropic materials. The test of the adequacy of such an approach would eventually rest with experimental substantiation.

Bowie[8] has pioneered in the application of complex variable and conformal mapping to crack problems. Basically, this concept involves the inverse mapping of the crack and its environment into the unit circle and its environment and the finding of a suitable stress function usually expressed as a single Laurent series. He has recently modified this approach, developing a technique which retains the character of the exact solution near the

crack tip but which incorporates the numerical simplifications associated with the collocation technique. In this Modified Mapping Collocation (MMC) technique he uses a relatively simple mapping function to detail only the crack tip region, but then enforces satisfaction of boundary conditions in a collocation sense. Figure 21 shows a selection of configurations which Bowie has treated using this technique. A more detailed representation of results for the specific case of non-uniform periodic edge cracks is shown in Figure 22. This shows the stress intensity, normalized, as a function of crack length ratios with crack "spacing" as a parameter. This problem was initially motivated by the gun tube problem wherein, due to the periodic bore rifling and the associated stress concentration factor, a periodic array of radial cracks generally form. It is important to know the pertinent stress intensity factors and particularly the interaction effects. The configuration of Figure 22 was an interim step toward this solution as a development of the cylindrical configuration. Concurrent with this exercise, however, Bowie and Freese have in fact carried out the case of the finite wall "ring" with radial cracks[9].

One of the major contributions associated with the MMC method is that it is appropriate not only for isotropic materials but also for anisotropic materials. It is a highly flexible technique. In fact, it has been programmed computationally ("ORTHO") so that wide classes of geometric configurations are readily accessible. Figure 23 shows the types of geometries which are treated by "ORTHO". The configurations on the left and right columns are intended to be rectangular; they are not restricted to square panels. Note the eccentricity of the cutouts or cracks and the various other plate configurations, i.e., circular and/or elliptical. And of course these can

be treated, as stated, either as isotropic or anisotropic plates.

It is noted also that the computational program "ORTHO" has been developed with a high emphasis on user orientation. "ORTHO" has been prepared by Freese so that it can be used by the engineer who has no - repeat NO - computer or analytical expertise to get stress intensity factors or stress distributions in these wide classes of problems. Typical training of a "user" of ORTHO entails no more than 5-10 minutes of instruction and the punching of two IBM cards if the material is isotropic and at most three IBM cards for anisotropic materials.

There are, however, limitations to this MMC method, and one such limitation is best discussed in terms of the example of Figure 24. Here are plotted the stress intensity vs crack length for a rectangular panel with edge cracks: a) with free ends under uniform tension; and b) with constrained ends under tension. Note that for the free end case, the stress intensity factor H (normalized) is relatively insensitive to the aspect ratio w/h once $w/h \geq 3$. Thus the greatest ratio one would have to consider in this case is then w/h = 3. Such a relatively short panel is easily tractable using a single power series expansion to represent the stress function in the entire region of the panel. On the other hand, for the constrained end case, note the sensitivity of the solution even at aspect ratios as high as w/h = 16. Though intuitively one would expect the solution for large w/h's to approach that of the infinite plates with free ends represented by the top curve w/h = 3, the solution has in fact not yet achieved that level even at w/h = 16. Solutions for large w/h are not very tractable using a single power series expansion to represent the stress function. Bowie et al [10] have therefore attacked this difficulty by considering such large or awkward

configurations as "partitioned" into smaller panels, and he then associates with each of these partitions a separate power expansion to represent the stress function in the respective areas. The solutions in each partition are then "stitched" together at the interfaces under imposed compatibility requirements in a collocation sense. Figure 25 shows the specific partitioning plan used in the present constrained ends problem. The symmetry of the problem was enforced by control of the coefficients and exponents of the Laurent series in I. Expansions of power series were also taken about the centers of regions of II and III. Compatibility of the solutions at the dashed lines was enforced. Using this approach, the solutions plotted in Figure 24 were readily obtained. Currently, Bowie is exploring the question of tradeoff between using a greater number of partitions vs phasing in of finite elements in order to optimize the size of the numerical system.

Bowie and Freese[11] and Lakshmikantham[12] were among the first investigators to recognize the marked effect of orthotropy in the crack problem. Figure 26 from Bowie and Freese[11] portrays some results of stress intensity factors vs crack length in an orthotropic finite plate over a range of aspect ratios c/b. Figure 27 taken from Lakshmikantham[12] more dramatically shows the effect of orthotropy on stress intensity factors. It is of particular interest to note the considerable difference between the orthotropic and the isotropic solution. Only at small crack lengths (λ) or equivalently for infinite sheets do the results merge. This perhaps accounts for the earlier misconception that material orthotropy did not influence stress intensity levels.

Gandhi[13] treated the more general case of arbitrary orientations of the crack and material orthotropy relative to the loading direction. Figure

28 shows some representative results for the special case of a square plate with a crack at 45^{o} and portrays the influence of material orientation on the normalized stress intensity factor for both the Mode I (crack opening) and Mode II (in-plane shear) conditions.

Lakshmikantham[12] has examined also the effect of stiffness in an infinite strip of orthotropic material with cracks. Results given in Figure 29 show the behavior with relatively low axial stiffness, intermediate and high axial stiffness. It is significant to note that for the low stiffness case the stress intensity curves for both isotropic and orthotropic panels display an ever increasing slope suggesting a rather unstable situation; i.e., when a crack starts to grow, it probably continues to expand in a catastrophic fashion. On the other hand, as the stiffness is increased, the slopes tend to level off, and in fact for the higher stiffnesses shown the curves take on negative slopes suggesting a more stable behavior, and in fact suggest the feasibility of crack arrest. In the case of the highest stiffness the orthotropic panel exaggerates this negative slope even more than the isotropic case suggesting its more favorable potential in a crack environment. Analysis of wide plates leads to the same general results[14].

Thus far in the discussion I've presented only our static considerations. We are also embarking on a serious effort to examine dynamic aspects of fractures, particularly in the low microsecond regime. Jones has recently completed the installation and preliminary testing of a 4-inch diameter light gas gun for use in plate slap studies. Figure 30 shows the facility in place. The breech assembly is to the left, the launch tube is approximately 26 feet long, feeds into t' .arget area, and thence into the large target recovery chamber clearly visible at the right end. Figure 31

is a schematic view of the system (oriented in juxtaposition to the previous figure). This system is capable of achieving impact pressures up to 570 kilobars and impact velocities up to 4000 feet per second dependent upon the specimen mass. The curves at the upper half of the figure suggest the type of data we expect to obtain; specifically, equations of state data including the Hugoniot yield value and fracture stress in a shock environment, i.e., spallation will be determined. "Projectiles" fired are in the form of thin discs supported during launch by a sabot arrangement. Targets are also disc-like. The curve at the upper left, though identified as impact velocity vs projectile thickness, can be interpreted as impact stress and pulse duration respectively, i.e., by varying the impact velocity, the stress level can be controlled, and by varying the projectile thickness, the pulse duration can be controlled.

Requirements for dynamic fracture criteria are motivated by our need to incorporate such data into penetration mechanics studies. Computer codes, particularly HEMP*, are being exploited by Mescall in treating the armor - projectile interaction problem. A typical computer-simulated result is shown in Figure 32. This shows the state of penetration some 0.78 micro seconds after impact. Since rotational symmetry is assumed, the view shown is a radial plane about the centerline of impact. The projectile impacting from the left at a velocity of 7,000 feet per second was initially a regular cylinder of steel; appreciable deformation is clearly visible. The armor system consisted of a front layer of boron carbide B_4C, a relatively brittle ceramic, and a backup plate of aluminum. Note the two failure areas of the forward ceramic plate. In particular, the failure by shear in this brittle

*HEMP - developed by M. L. Wilkins, Lawrence Livermore Labs.

ceramic was predicated on a maximum plastic effective strain. This may appear puzzling, i.e., that plastic - strain is tolerated in such a material. On the other hand, it must be kept in mind that this is possible only because of the excessively high hydrostatic pressure existing in the region of impact. Under such ambient pressures brittle materials may deform plastically. The actual strain to fracture was in fact taken to be a function of the pressure/effective stress ratio. The exact nature of this function is not known in detail; rather only a few points are well characterized. More detailed information is needed. We will be seeking some data to fill this gap.

In the second area of failure, identified as tension failure, it was determined that this region was subjected to tensile stresses in excess of 30 kilobars. This is vastly in excess of the anticipated fracture strength of the material, but no hard data are available on these values - so once again it is evident that fracture data - characterization of these relatively brittle materials under short duration-high intensity tension pulses - is required if we are to reliably predict performance in the penetration environment.

III. FATIGUE

Our studies in fatigue have been somewhat more limited than the fracture investigations. We have one team of investigators exploring the crack initiation and another the crack propagation stages of fatigue. The emphasis currently in both these efforts relates to behavior of metals. Composite behavior under fatigue is only beginning to receive more of our attention.

The crack initiation study led by Papirno is aimed at acquiring some

quantitative observations of crack initiation mechanisms and then at the establishment of pragmatic criteria for crack initiation which can be integrated with cyclic crack propagation and ultimate fracture criteria to predict failure of components.

As a preliminary step aimed at defining and quantifying "initiation", Papirno et al [15][16] have developed an automatic system to take flash photomicrographs at roots of notches in flat, doubly-notched specimens during low cycle fatigue tests. A schematic view of the notch region of the specimen is shown in Figure 33. A wide range of theoretical elastic stress concentration factors K_t is readily obtained with this configuration. The present study has been limited to date to a range of K_t from 1.5 to 5.0. Figure 34 shows the arrangement of apparatus for the photomicrography. It is noted, of course, that with the doubly notched specimen of Figure 33 and the dual photographic assembly, each test constitutes two sets of data, one for each notch.

The photographic apparatus is synchronized with the loading machine to take photomicrographs on 35mm film at preprogrammed cyclic intervals without arresting the cyclic loading procedure. This is continued until a well defined crack has formed. The developed film is then examined and the crack is traced backward in time frame by frame. A crack was judged to have just initiated when it was visible in one frame but not in the frame just preceding. Resolution of cracks with a surface length of .001 inch and an opening of .0001 inch was easily effected using projected images. Repetition rates for recording photos was generally 100 cycles, though a limited number of tests at very low cycle life were photographed at 50 cycle intervals. Furthermore, the photomicrographs were taken at maximum load in the cycle, thus

making the cracks more visible. These techniques permitted confident identification of crack initiation to within ±50 or ±25 cycles.

Figure 35 shows a selected sample of photomicrographs of the notch base after various number of cycles. These were taken from a long sequence of films. The particular specimen involved had an initial elastic stress concentration factor of K_t of 4, and the figure illustrates one form of cracking behavior where a number of individual cracks initially form and then coalesced into one dominant crack and a few dormant cracks. The initiating cracks are more clearly visible in the negatives. The circle outlines the site of the first crack. Generally, though not consistently, the initial cracks developed near the mid thickness. Furthermore, the growth pattern was not always one of several initiation cracks coalescing into one dominant crack. More generally - and this depends not only on the materials but also on the initial stress concentration factor, and the load (and quite probably on the gradient of stress) - only some of the initial cracks coalesced to form the dominant crack; others remained isolated and dormant. Figure 36 shows a typical count of the cracks visible at the notch base as a function of cycles. It is noted that both notches developed first cracks at about 1600-1700 cycles; subsequently, as many as six independent cracks were observed on one side (four on the other). Eventually a dominant crack became evident (at about 5000 cycles) though the dominant crack was not the only crack present. The indicated points correspond to the cycle count at which the crack intercepted the face of the specimens. In this particular case one crack initiated at the edge; the other required some 3000 cycles before reaching the edge. This, of course, highlights the difficulty associated with interpretations based solely on observations made on the faces of notched specimens. Initial testing was carried out with zero - tension loading. Additional tests

are being done over the range of compression to tension.

The limited tests carried out to date have been on an AISI 4340 steel. Selection was not based on an inherent interest in this particular material but rather it was desired to use, as a vehicle for study of and development of pragmatic design criteria, a well characterized and structurally significant material. Other more advanced materials such as Transformation Induced Plasticity (TRIP) steel, for example, are, however, to be explored.

As an adjunct to these studies and in anticipation of the more detailed continuum treatment of the elastic-plastic behavior of the notched material, Papirno and Campo[17] have developed a technique for extending the strain range of conventional strain gages. Figure 37 shows the arrangement used. With this procedure, cyclic strains of the order 1 - 3% are conveniently measured and monitored. Satisfactory results have been achieved for as many as 5000 cycles at strain levels $\geq$ 1.5%.

In exploring crack propagation behavior, Matthews et al[18] have recently reported effects of sudden or step changes in the stress intensity factor on propagation rates. They tested sheet specimens of AISI 4340 steel quenched and tempered to an ultimate tensile strength of 191 ksi. The specimen configuration along with some results are sketched in Figure 38. Specimens 0.157 and 0.025 inches in thickness were cycled (tension - tension; $K_{min}/K_{max} = 0.1$) in a dry air atmosphere using a closed loop hydraulic testing machine. The load was reduced incrementally at crack extension intervals of 0.025 inches to maintain a quasi-constant ΔK loading to within $\pm 1.3\%$ of the desired level. This constant ΔK was maintained until the growth rate reached a steady state. At this point the load level was raised to obtain a new higher ΔK level. The cyclic loading was reapplied and the crack growth rate

again observed. During this second stage, also, the load was adjusted periodically to maintain the constancy of the augmented ΔK level as the crack progressed. The crack length was monitored at frequent cyclic intervals using a traveling microscope on both sides of the specimen. Typical results shown in Figure 36 show a rather significant transient augmentation of the crack growth rate well beyond that steady state level which could be expected based solely upon the second stage stress intensity factor. This is an unconservative trend and could have serious consequences in critical designs if not recognized and taken into consideration. We are attempting to formulate models which will adequately and conveniently account for this behavior. Studies will also include observation of behavior when the second stage ΔK range is decreased from the level of the first stage.

In a separate but related effort to try to provide a useful tool for prediction of steady state crack propagation rates over the wide spectrum of ΔK values from threshhold to critical levels, Bluhm et al[19] have formulated the following tentative and empirical relation which does in fact account for, at least qualitatively, transitions in crack propagation behavior over these extremes of ΔK levels.

$$\frac{da}{dN} = C \frac{\left(\frac{\Delta K}{\Delta K_o} - 1\right)^m}{\left(1 - \frac{K_{max}}{K_c^*}\right)^n} \qquad (2)$$

where C, m, n are constants,

ΔK_o is the threshhold level of the stress intensity factor range corresponding to K_{max},

K_{max} is the maximum cyclic value of the stress intensity factor,

K_c* is an appropriate fracture toughness value dependent upon K_{max}, plate thickness, yield strength, etc. and based upon the model for thickness effect described by Bluhm[20].

We have not, however, had the opportunity yet to experimentally verify the range of validity of this relation. The form of this relation is of particular interest in that it displays a non-uniqueness of da/dN for a given ΔK; because the thickness effect is explicitly reflected in K_c*, the da/dN curve takes on the characteristic behavior sketched in Figure 39.

Beeuwkes[21] has examined the more restricted crack propagation "law" defined in the general form

$$\frac{da}{dN} = C\ \overline{\Delta K}^2 \tag{3}$$

Replacing $\overline{\Delta K}^2$ by its stress equivalent $\overline{\Delta\sigma}^2 a$ (for a small crack), this equation can be written as follows*

$$\frac{da}{a} = C\ \overline{\Delta\sigma}^2\ dN \tag{4}$$

and by integration,

$$\ln a = \ln a_o + C\ \overline{\Delta\sigma}^2\ (N - N_o) \tag{5}$$

*Finite width corrections using the Feddersen secant correction factor were actually considered by Beeuwkes and led to Equation (a) below instead of Equation (4) above where $C_i\ (\frac{\pi a}{W})$ is the cosine integral. (Nevertheless one is led to the same conclusions.)

$$C_i(\frac{\pi a}{W}) = C_o + C_1\overline{\Delta\sigma}^2\ \ (N - N_o) \tag{a}$$

This form of a versus N leads to a straight line prediction for ln a versus N. In the plotting of extensive data Beeuwkes noted, however, that the data in fact were better represented by a series of intersecting straight lines with each successive segment having approximately twice the slope of the preceding segment. Typical data are shown in Figure 40. These transitions were not always associated with observable gross changes in fracture surface appearance. This, however, is being explored further.

When da/dN is appropriately determined graphically from this data one is consistently led to a discontinuous log-log plot of da/dN versus ΔK as shown in Figure 41. Of particular interest is Beeuwkes' observation that the slopes of these disjointed segments are statistically identical and approximately 2 which is consistent with the exponent of Equation 3. However, it is further noted that the mean "curve" going through all the segments has the slope 4 which has frequently been identified as the appropriate power. Some 100-200 crack propagation curves from a dozen or so investigators have been analyzed by this treatment and almost without exception behave in identical fashion.

IV. PERIPHERAL STUDIES

Contributing to and complementing both the fracture and fatigue studies, is a program being carried out by Lenoe aimed at defining constitutive relations for various classes of structurally important materials. He has initiated a series of creep and relaxation tests on unidirectional fiber reinforced composites. To date the materials studied have been S glass, boron, Thornel 50 and Mod Mor II reinforced epoxies over the temperature range from room temperature to 400^{o}F. Representative creep and relaxation data are

shown in Figures 40 and 41. Additional materials to be investigated will include E glass in various epoxy resins, PRD-49, as well as metal and ceramic matrix composites. Studies will also be extended to include angle ply configurations. Testing will be in longitudinal and transverse tension, torsion and in-plane shear.

A major objective of this investigation, aside from the data collection aspect, is to examine various theoretical approaches to creep prediction from relaxation response (or vice versa) and to provide techniques for estimating angle ply behavior from known behavior of unidirectionally reinforced composites. The most appropriate of these approaches might then be recommended as an engineering analysis procedure.

Additionally, Chou has been examining the dynamic behavior of several polymers; specifically the stress-strain curves at strain rates up to approximately 10^3 per second, particularly in compression, were determined. Preliminary results revealed that one polymer, polypropylene, displayed rather surprisingly a maximum load feature; this is usually observed only in tension specimens. In attempting to account for this behavior and since this material was known not to have a phase transition at the nominal stresses and temperature of the test, Chou, anticipating a possibly significant temperature rise, instrumented a number of specimens with imbedded thermocouples and repeated the tests.

Results of several representative compression tests on the polypropylene are shown in Figure 44. Three stress-strain curves are shown for strain rates from 2×10^{-3}/sec to 1530/sec. Only the curve for the high strain rate shows this maximum load characteristic. In the same figure are plotted the recorded temperatures. It is noted that at the two higher strain rates,

a marked knee in the temperature, stress curve is evident. At the highest strain rate ($\dot{\varepsilon}$ = 1530/sec) this knee occurs at the maximum load point. We are not sure yet of the mechanisms interacting to generate the temperature rise and/or the peaking behavior of the stress-strain curve.

Our interest here is motivated by the practical implication with respect to the consequences of such behavior in these materials if used in personnel armor or more generally as a matrix material in composites.

V. CONCLUSION

Summing then, I have briefly described a sampling of the experimental and analytical studies at AMMRC relating to fracture and fatigue and have even more briefly made reference to some of our activities in constitutive relationships. Time limitations have precluded more detailed description of the foregoing or reference to other relevant studies, such as the following:

Beeuwkes	on	Fracture Criteria and Crack Growth Law.
Baratta	on	Design of Specimens for Fracture Testing of Brittle Materials.
Lenoe	on	Integration of Specimen Configurations and Fracture Considerations in Reliability Considerations.
Papirno	on	Elastic-Plastic Notch Behavior.
Matthews	on	his "Collection of Plane Strain Fracture Toughness Data".

Interested personnel are invited to contact the investigators directly for further elaboration.

I would like to acknowledge the staff of the Theoretical and Applied Mechanics Research Laboratory as being the prime generator of the studies I have presented and to repeat that my role here today has been one strictly of reporter. Thank you.

REFERENCES

[1] SLEPETZ, J. M., "Fracture of Unidirectional Composite Compact Tension Specimens", AMMRC report in preparation.

[2] CHIANG, F. P. and SLEPETZ, J. M., "A Note on Crack Length Measurement in Composite Materials by Moire Method", AMMRC Technical Note in preparation.

[3] OPLINGER, D. O., "Edge Effects in Angle Ply Composites", AMMRC TR 71-62, dated Dec 1971.

[4] OPLINGER, D. O., CHIANG, F. P. and PARKER, B.S., "Experimental Studies of Edge Effects in Composites", AMMRC Technical Report in preparation.

[5] GANDHI, K., "Two Dimensional Analysis of Lap Joints", AMMRC technical report in preparation.

[6] OPLINGER, D. O. and GANDHI, K, "Analytical Study of Failure Strength of Bolted Joints in Layered Composites", AMMRC technical report in preparation.

[7] RICH, T., "Structural Mechanics of Battle Damage". Report in preparation.

[8] BOWIE, O. L., "Solution of Plane Crack Problems by Mapping Technique", Methods of Analysis and Solutions of Crack Problems, Edited by George C. Sih, Wolters Noordhoff, 1972.

[9] BOWIE, O. L., and FREESE, C. E., "Elastic Analysis for a Radial Crack in a Circular Ring", AMMRC Report AMMRC MS 70-3, Sep 70.

[10] BOWIE, O. L., FREESE, C. E., and NEAL, D. M., "Solution of Plane Problems of Elasticity Utilizing Partitioning Concepts", 1972, submitted for publication.

[11] BOWIE, O. L., and FREESE, C. E., "Central Crack in Plane Orthotropic Rectangular Sheet", Int J. of Fracture Mechanics, Vol. 8, No. 1, March 1972.

[12] LAKSHMIKANTHAM, C., "Analysis of Transverse Cracks in Stiffened Fiber-Composite Strips Under Tension", AMMRC Report No. TR 71-1, Jan 71.

[13] GANDHI, K. R., "Analysis of an Inclined Crack Centrally Placed in an Orthotropic Rectangular Plate", AMMRC TR 71-31, Aug 1971.

[14] LAKSHMIKANTHAM, C., "Analysis of Cracks in Wide Orthotropic Plate with Longitudinal Stiffeners", AMMRC TR 71-29, Aug 71.

[15] PAPIRNO, R., and PARKER, B. S., "Fatigue Crack Initiation Using Flash Photomicrography - Part I - Experimental Equipment and Procedure", AMMRC TR 71-51, Dec 71

[16] PAPIRNO, R. and PARKER, B. S., "Fatigue Crack Initiation Using Flash Photomicrography - Part II - Experimental Results" (in preparation).

[17] PAPIRNO, R. and CAMPO, J., "A Strain Gage Configuration for High Level Cyclic Strain", AMMRC TN 71-6, Dec 71.

[18] MATTHEWS, W. T., BARATTA, F. I. and DRISCOLL, G. W., "Experimental Observation of a Stress Intensity History Effect Upon Fatigue Crack Growth Rate", Int J1 of Fracture Mechanics 7 (1971).

[19] BLUHM, J. I., BARATTA, F. I., DRISCOLL, G. W., and MATTHEWS, W. T., "Crack Propagation Rates at Extremes of Stress Intensity Factor", Unpublished notes, Nov 69.

[20] BLUHM, J. I., "A Model for the Effect of Thickness on Fracture Toughness", Proc ASTM. Vol 61 (1961) 1324-1331.

[21] BEEUWKES, R. Jr., Discussion held with Beeuwkes April/May 1972; Technical Note being prepared for publication.

CONSTITUTIVE RELATIONS

FATIGUE

FRACTURE

WEAR AND EROSION

STRUCTURAL DYNAMICS

STRUCTURAL INSTABILITY

STRESS AND DEFLECTION

STRUCTURAL OPTIMIZATION

Figure 1. Solid Mechanics Responsibility at AMMRC

Compact Tension Specimens

S-Glass/Epoxy

Thornel-50/Epoxy

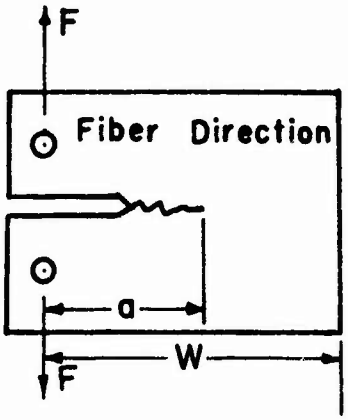

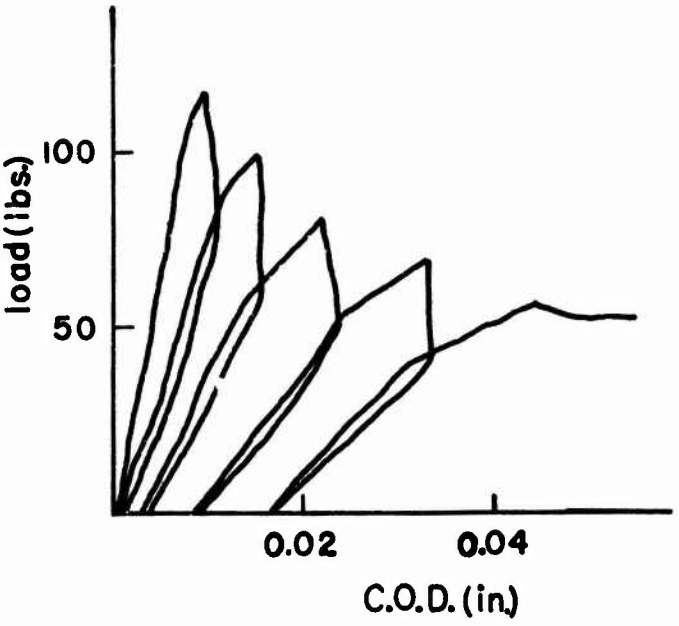

△ S-Glass/Epoxy

○ Graphite/Epoxy

$$G_c = \frac{F^2_{max}}{2t}(dC/da)$$

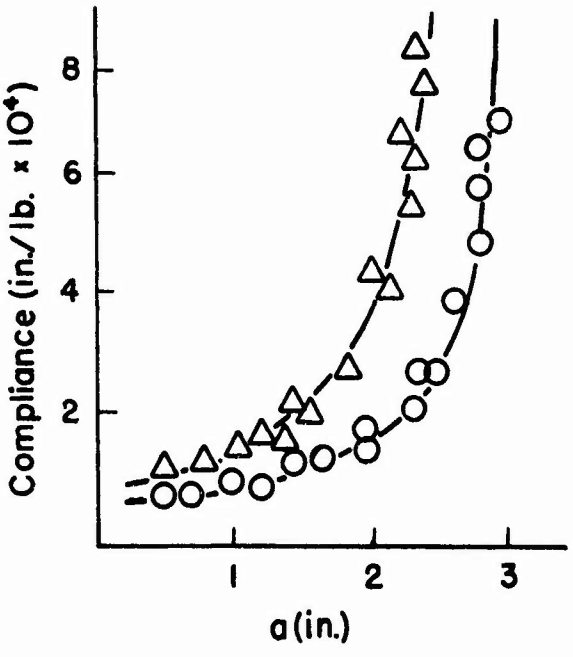

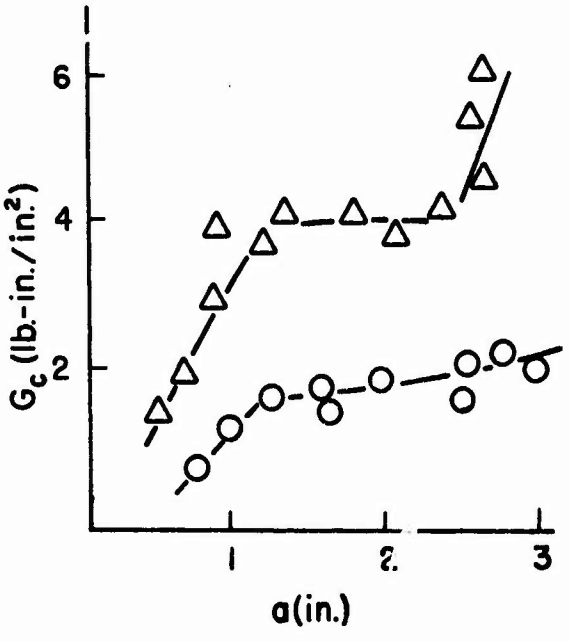

Figure 2. Fracture Mechanics in Composites, An Overview

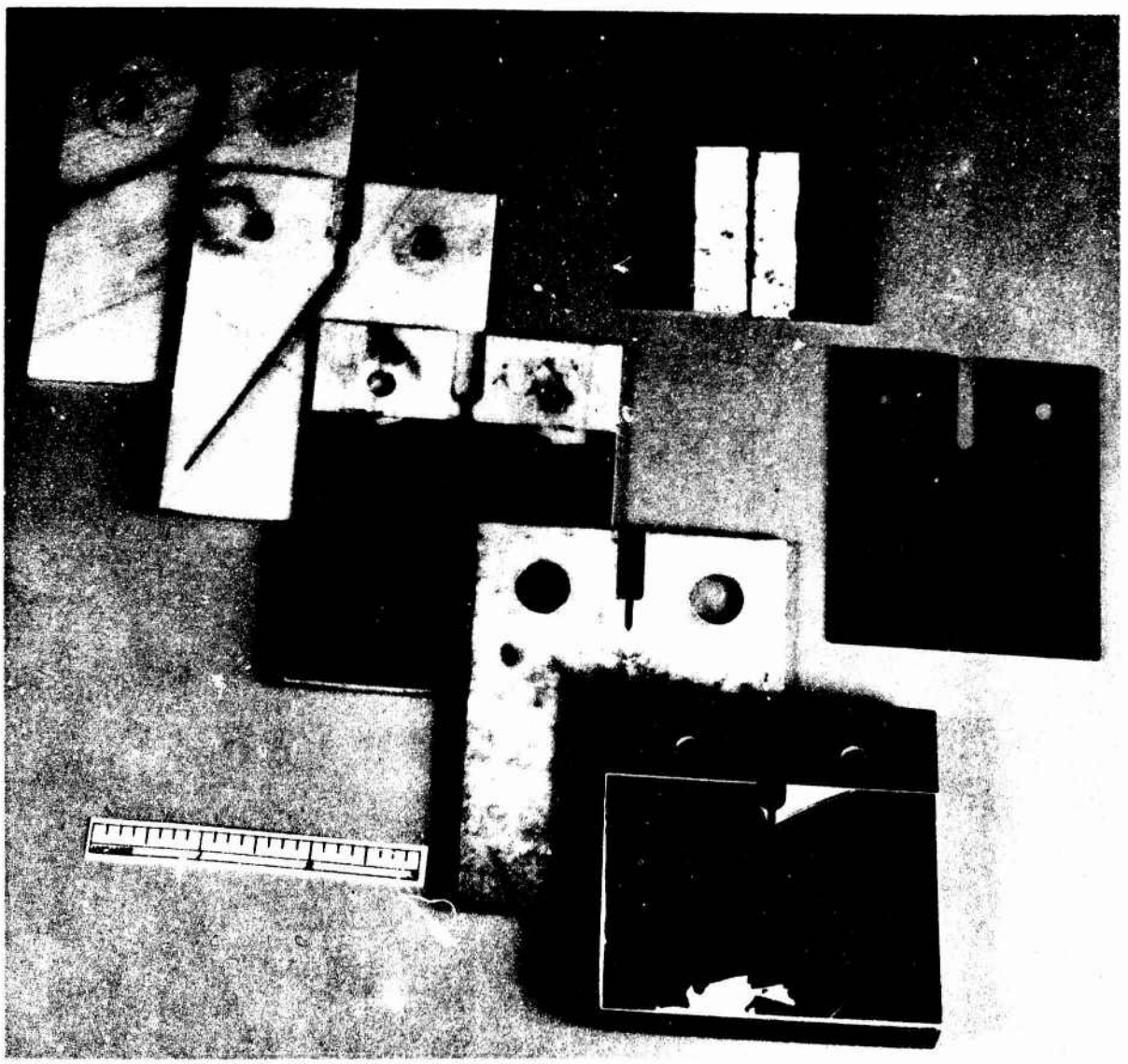

19-066-801/AMC-72

Figure 3. Compact Tension Specimens for Composite Fracture Studies

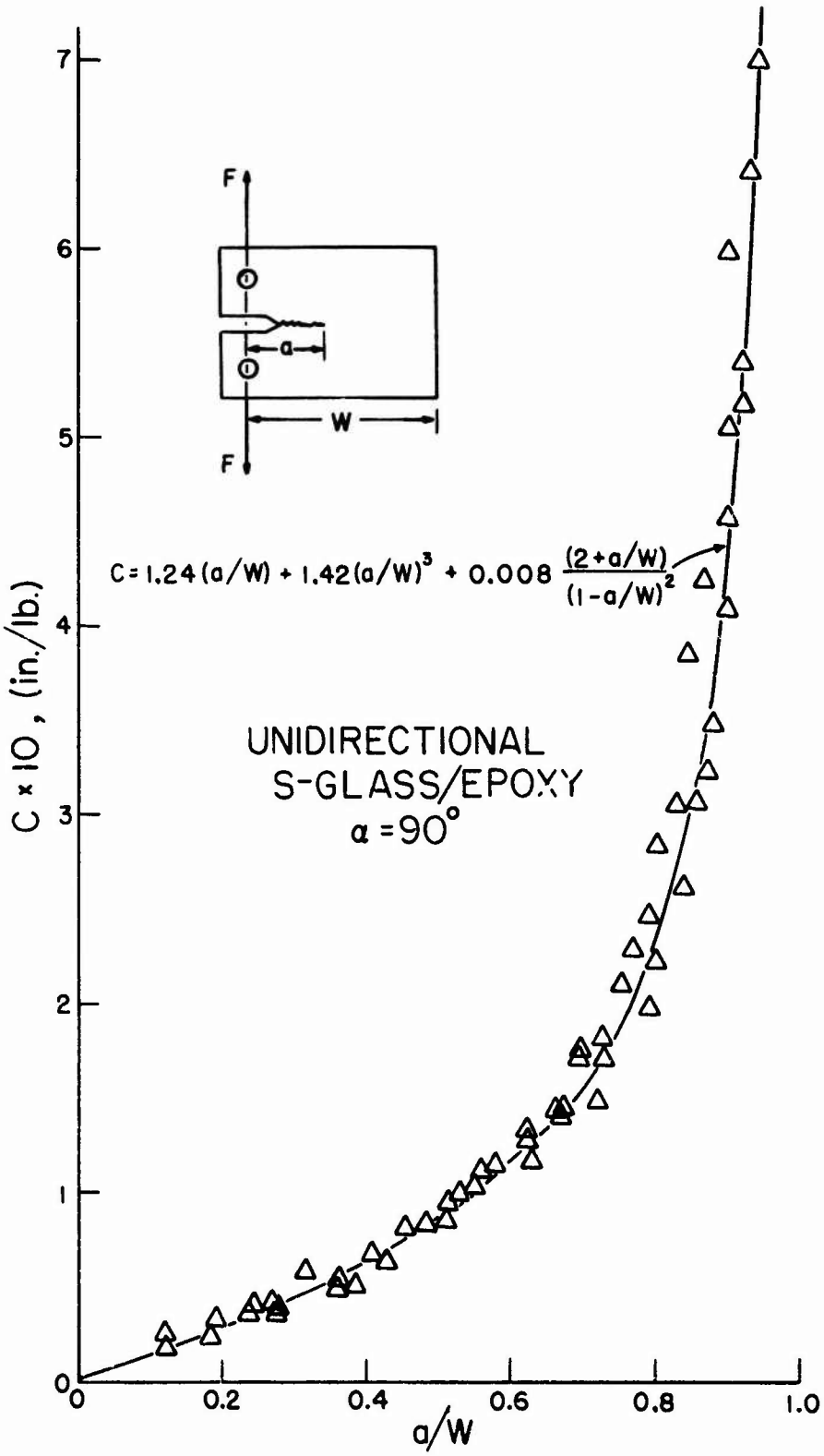

Figure 4. Compliance Data for Unidirectional S-Glass/Epoxy

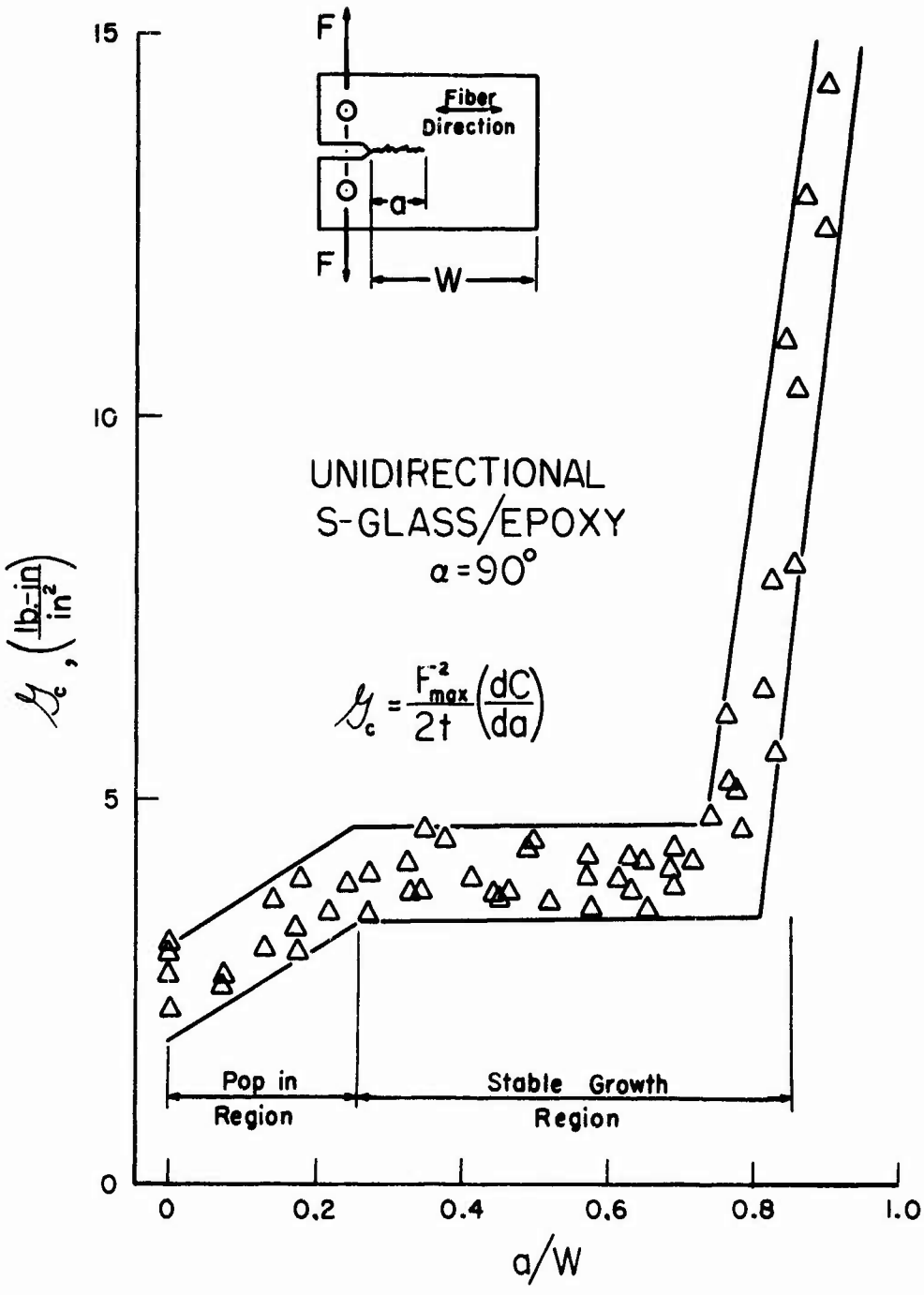

Figure 5. Fracture Toughness for Unidirectional S-Glass/Epoxy

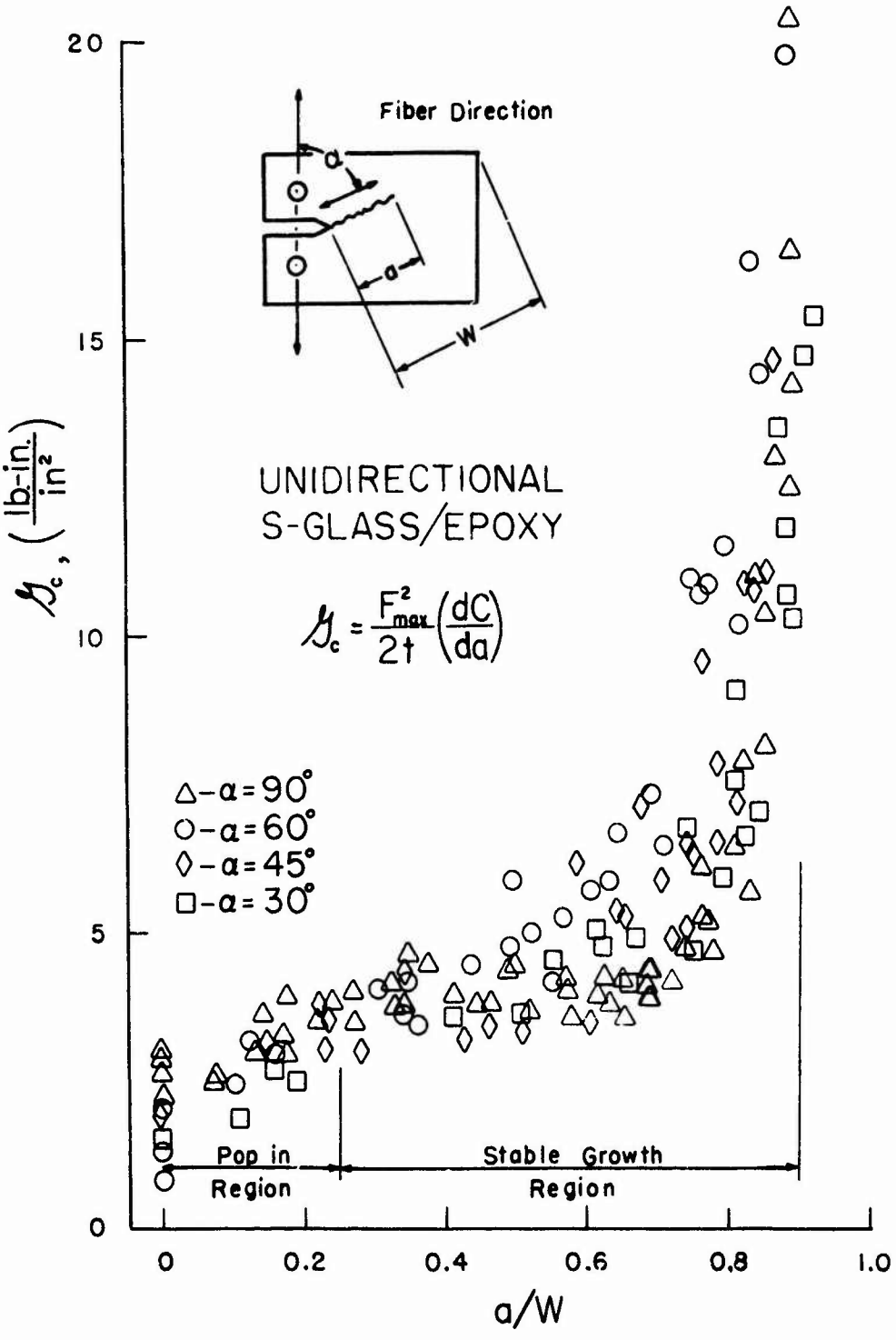

Figure 6. Fracture Toughness for Unidirectional S-Glass/Epoxy, Effect of Fiber Direction.

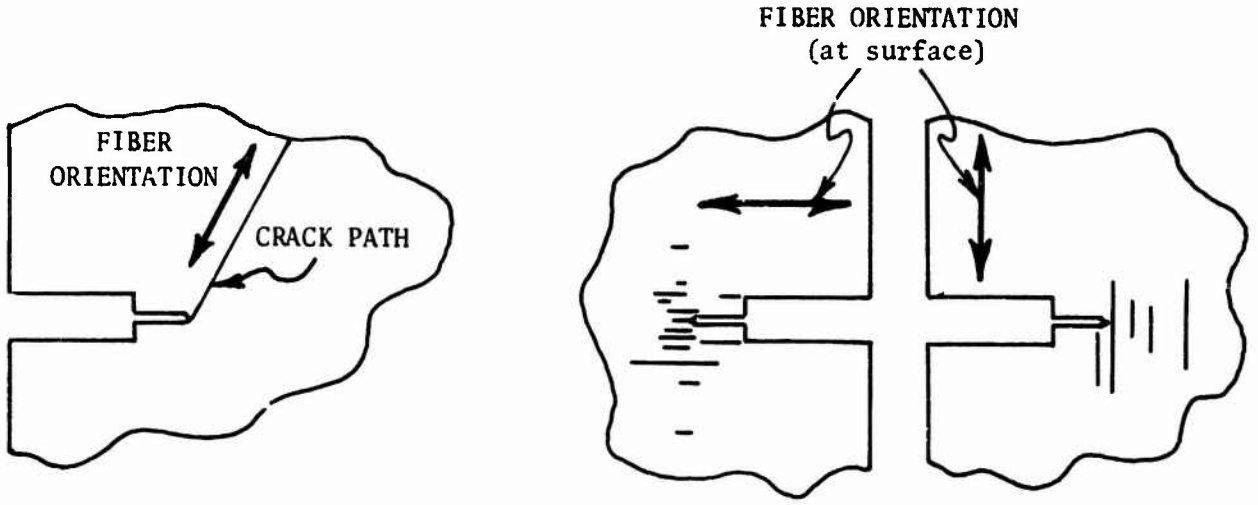

a. Unidirectional fiber specimen.

b. Side views of a cross ply specimen.

Figure 7. Effect of Fiber Orientation on Crack Pattern

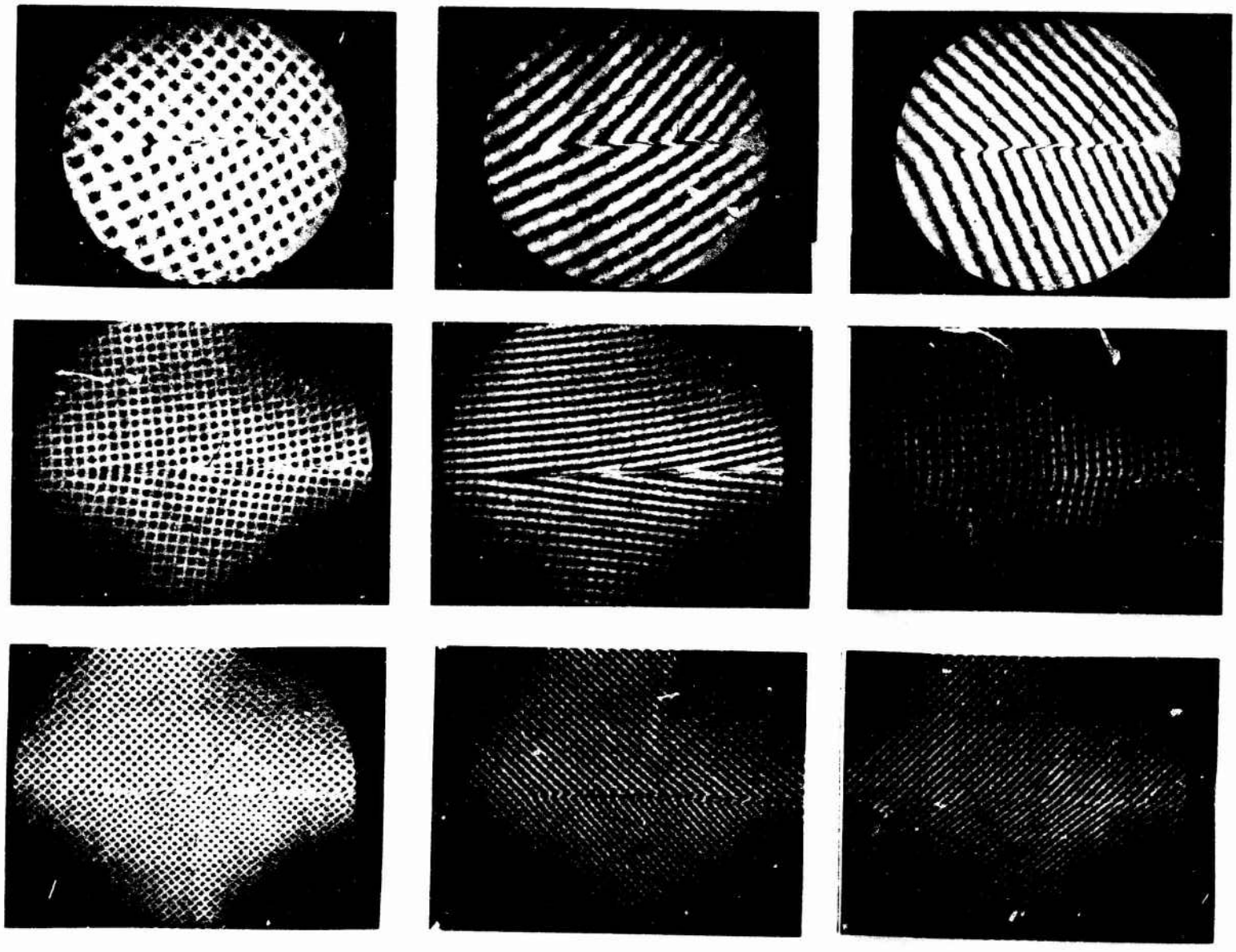

Figure 8. Moiré Interference Pattern at Crack Tips in Unidirectional Composites

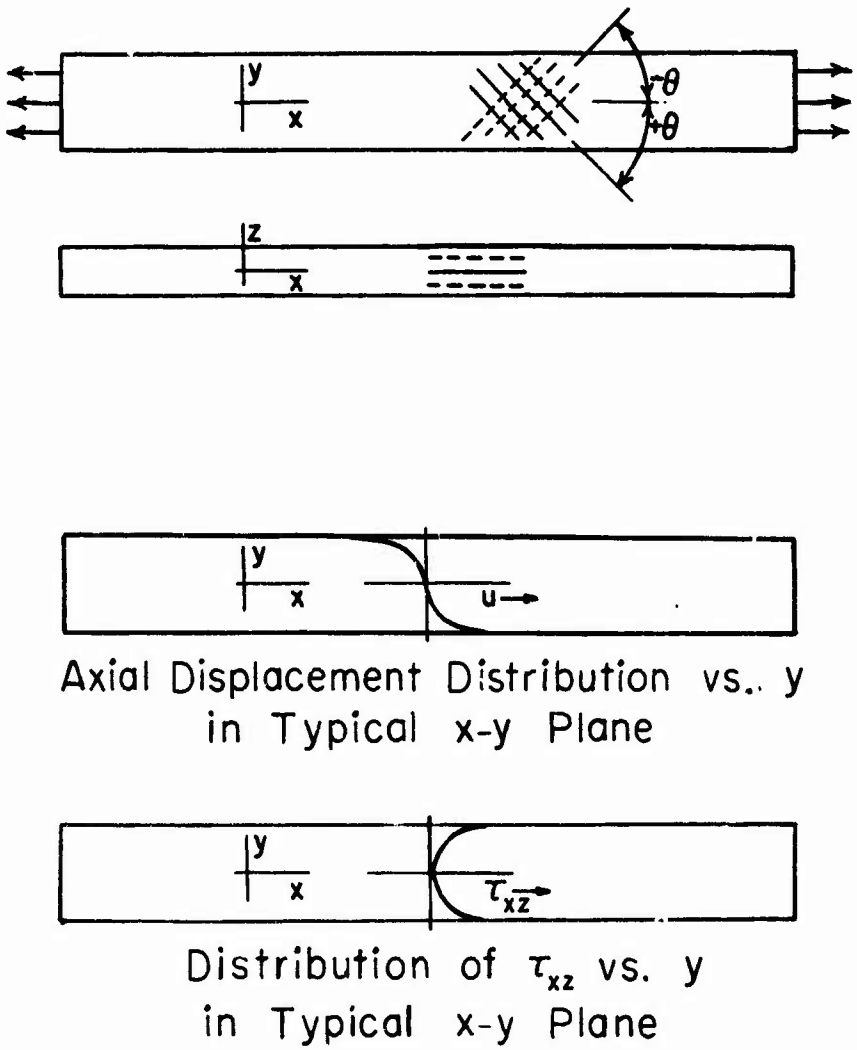

Figure 9. Deformation and Interlaminer Shear Distributions in Angle Ply Composites

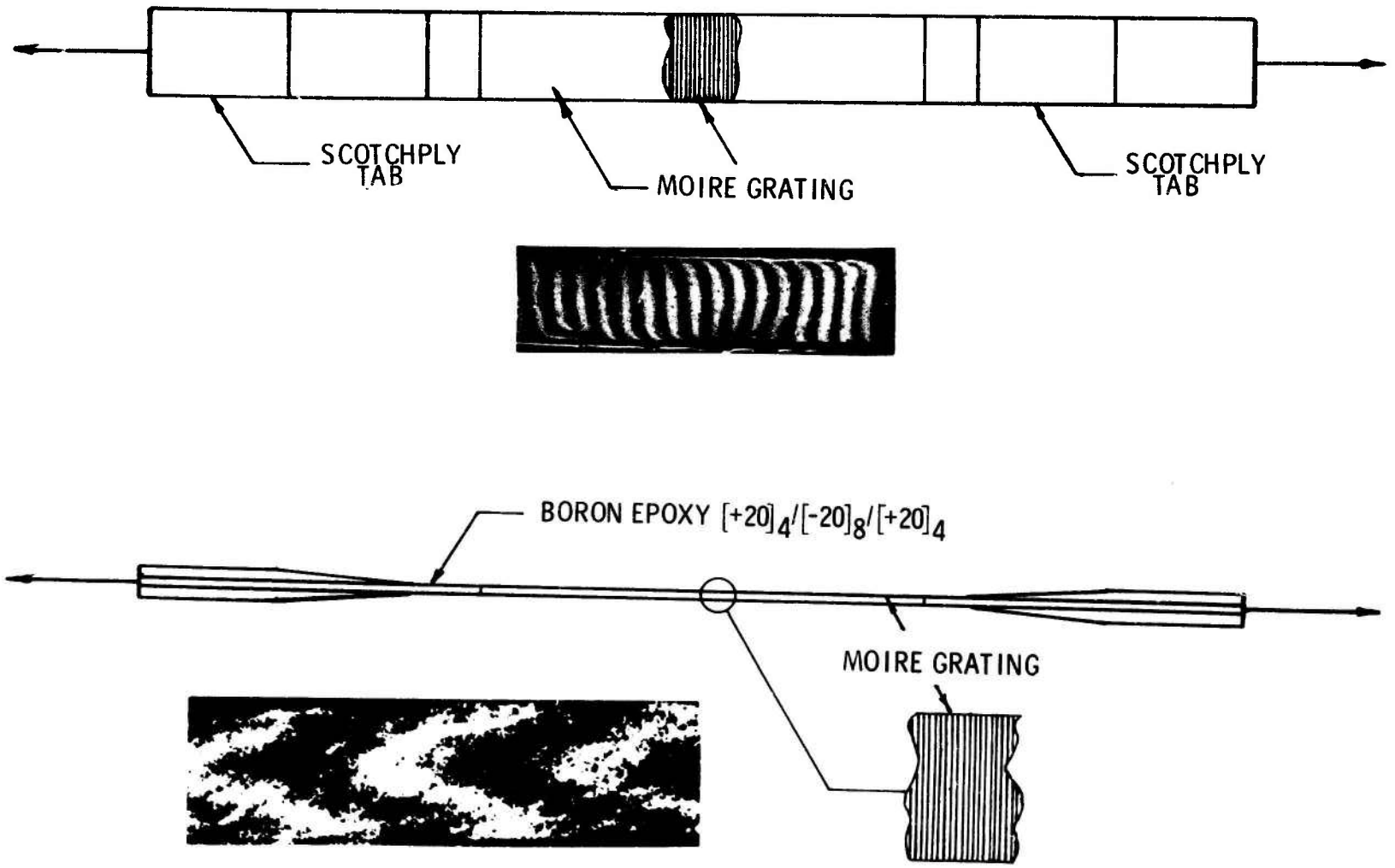

19-066-553/AMC-72

Figure 10. Moiré Patterns in ±20 Degree Boron Epoxy Tensile Specimen

19-066-519/AMC-72

Figure 11. Moiré Patterns in ±20 Degree Boron Epoxy Tensile Specimen - (Effect of Load Level)

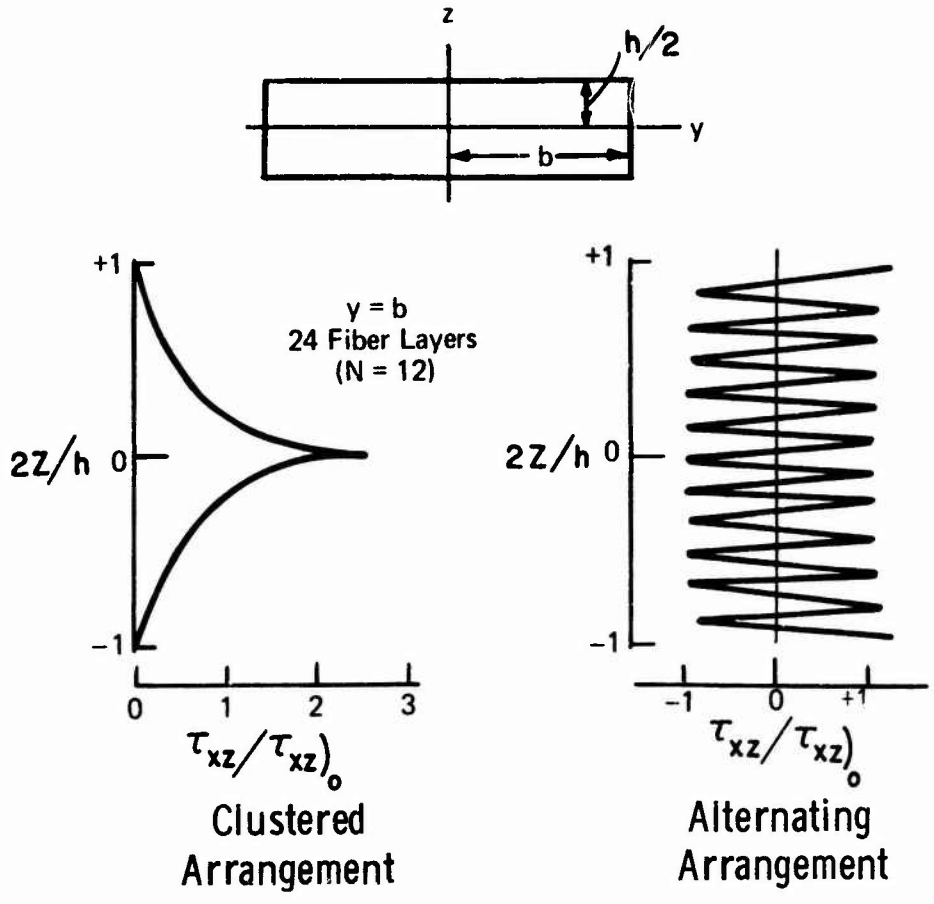

Figure 12. Distribution of Interlaminar Shear Stress τ_{xz} at Free Edge (y=b) of Angle Ply Strip under Tension.

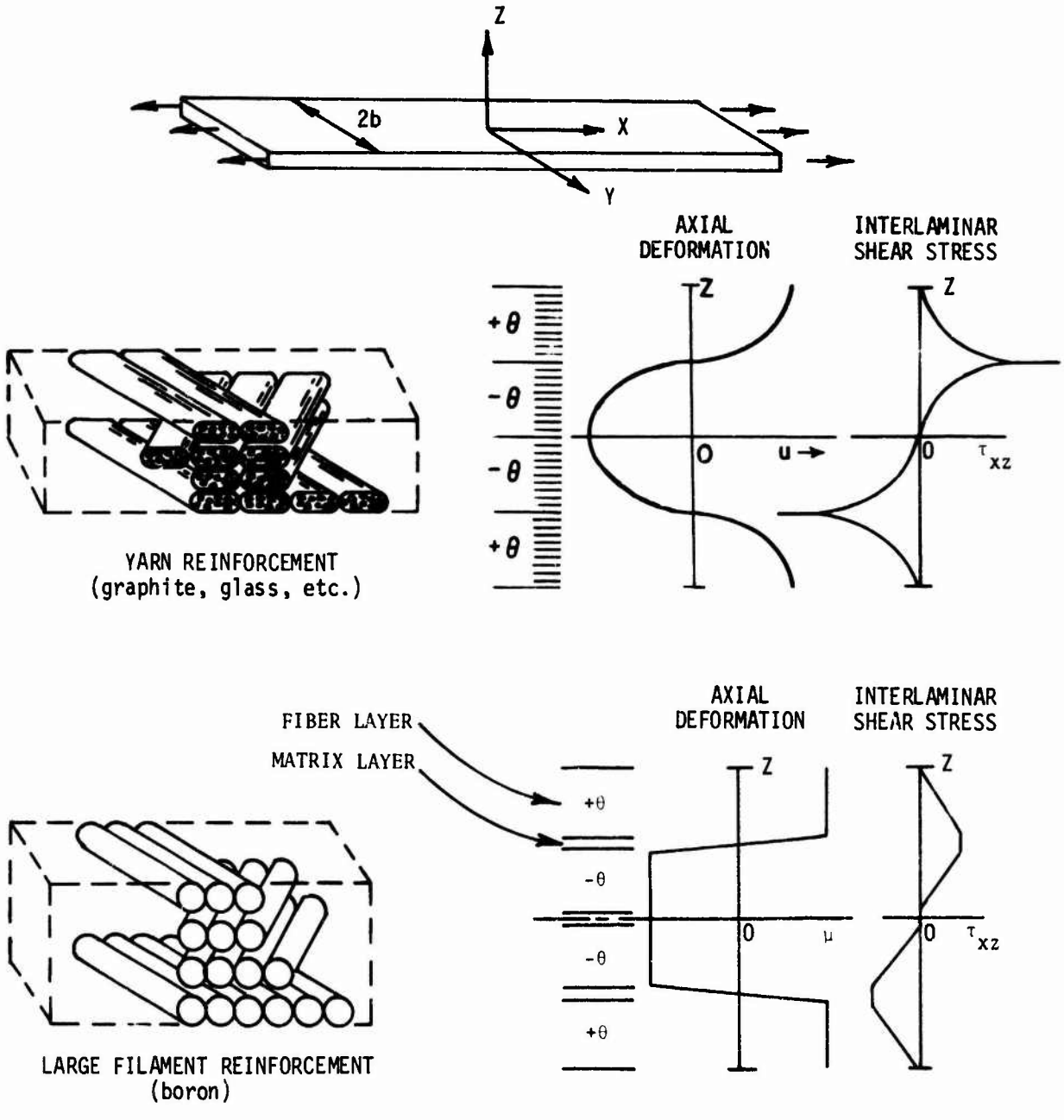

Figure 13. Effect of Filament Structure on Deformation and Interlaminar Shear Stress at Edge y=b

STACKING SEQUENCES

C (CLUSTERED)

$4/+\theta$
$8/-\theta$
$4/+\theta$
} 16 Layers

A (ALTERNATING)

$+\theta$
$-\theta$
$+\theta$
} 8 Layers

PLY ANGLE (θ)	BORON EPOXY SEQUENCE		GRAPHITE EPOXY SEQUENCE	
	A	C	A	C
$\pm 10^0$	X	X	X	X
$\pm 20^0$	-	X	-	-
$\pm 30^0$	-	-	X	X
$\pm 45^0$	X	X	X	X

Figure 14. Matrix of Experiments

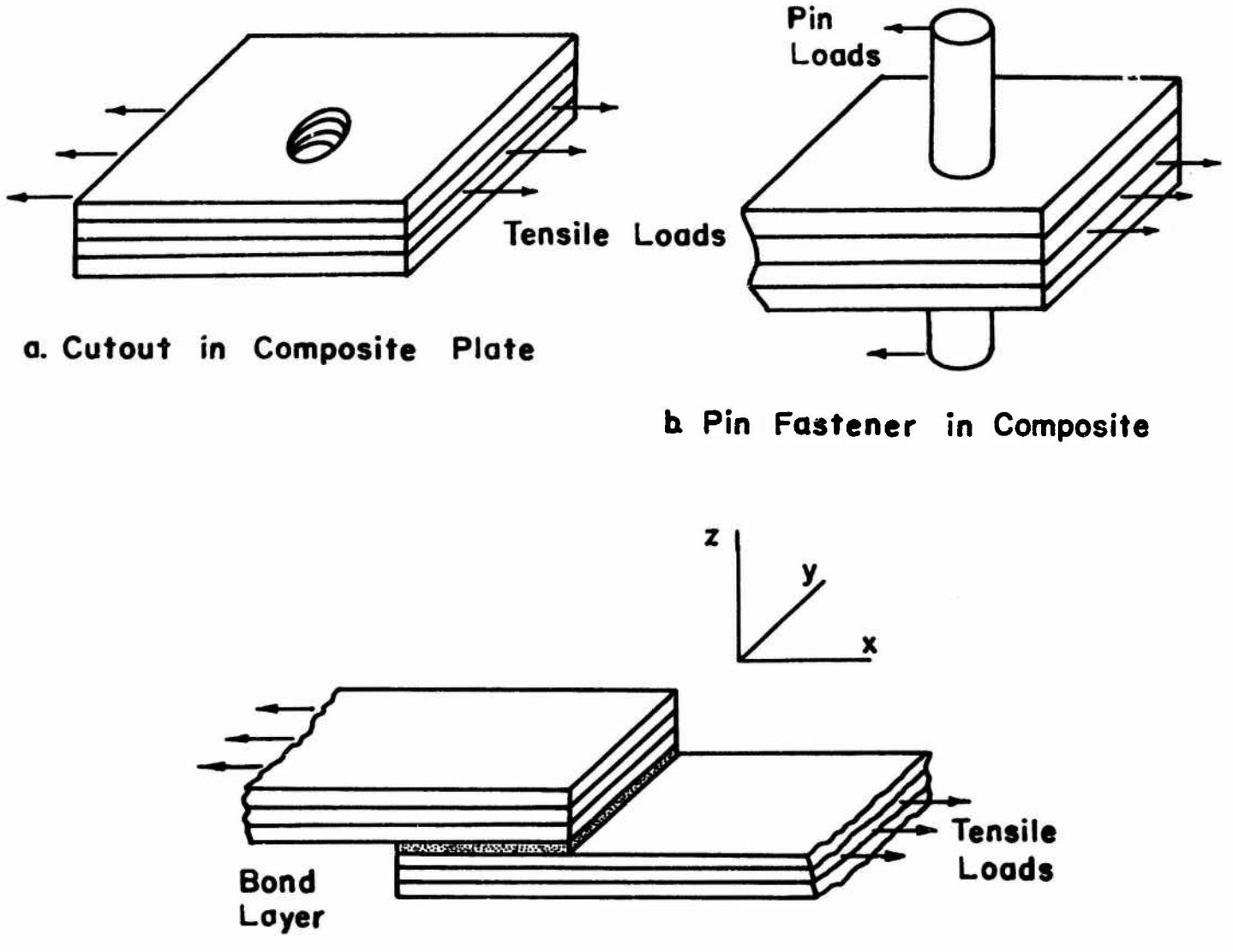

Figure 15. Typical Layered Structural Configuration under Study in Connection with Joints

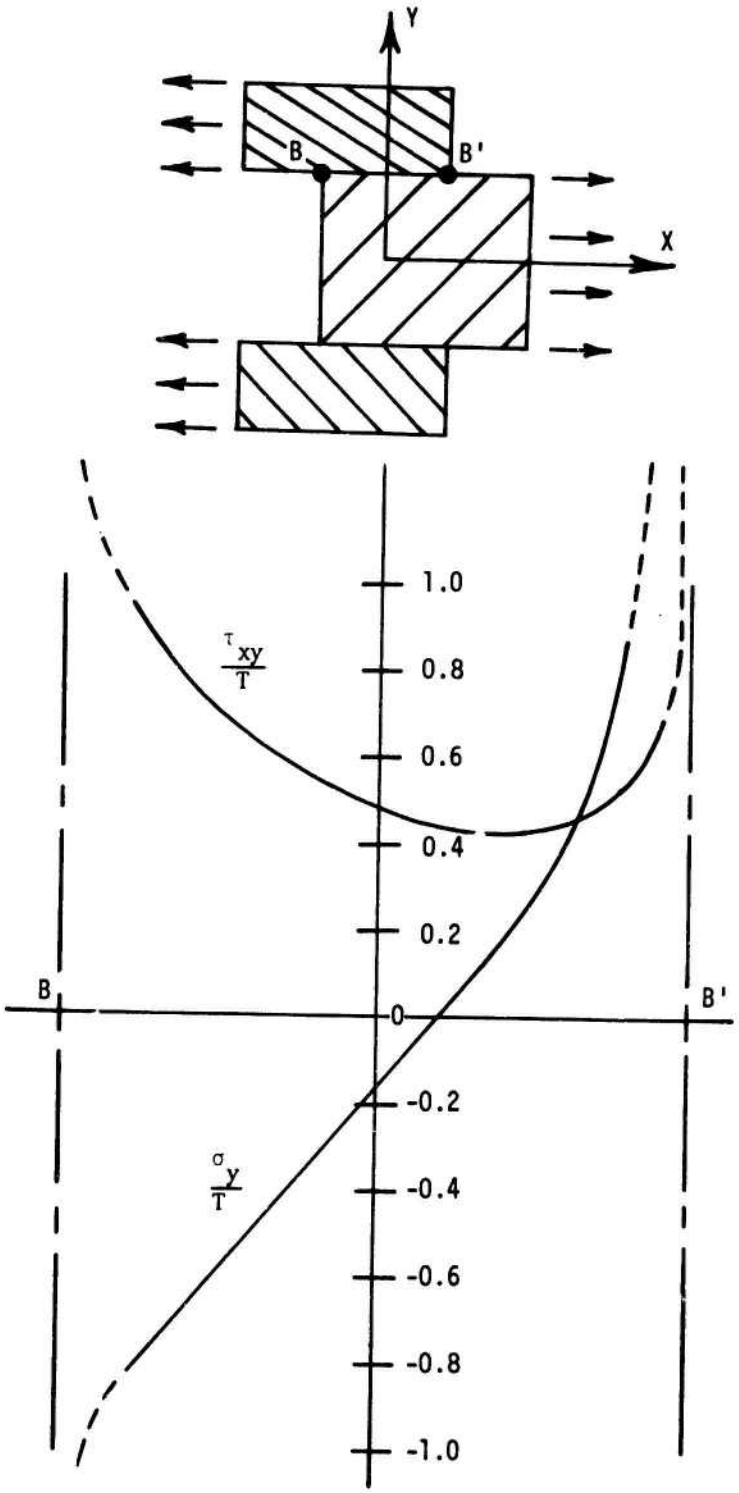

Figure 16. Representative Stress Distribution Along Adhesive Line (Plane Strain Solution)

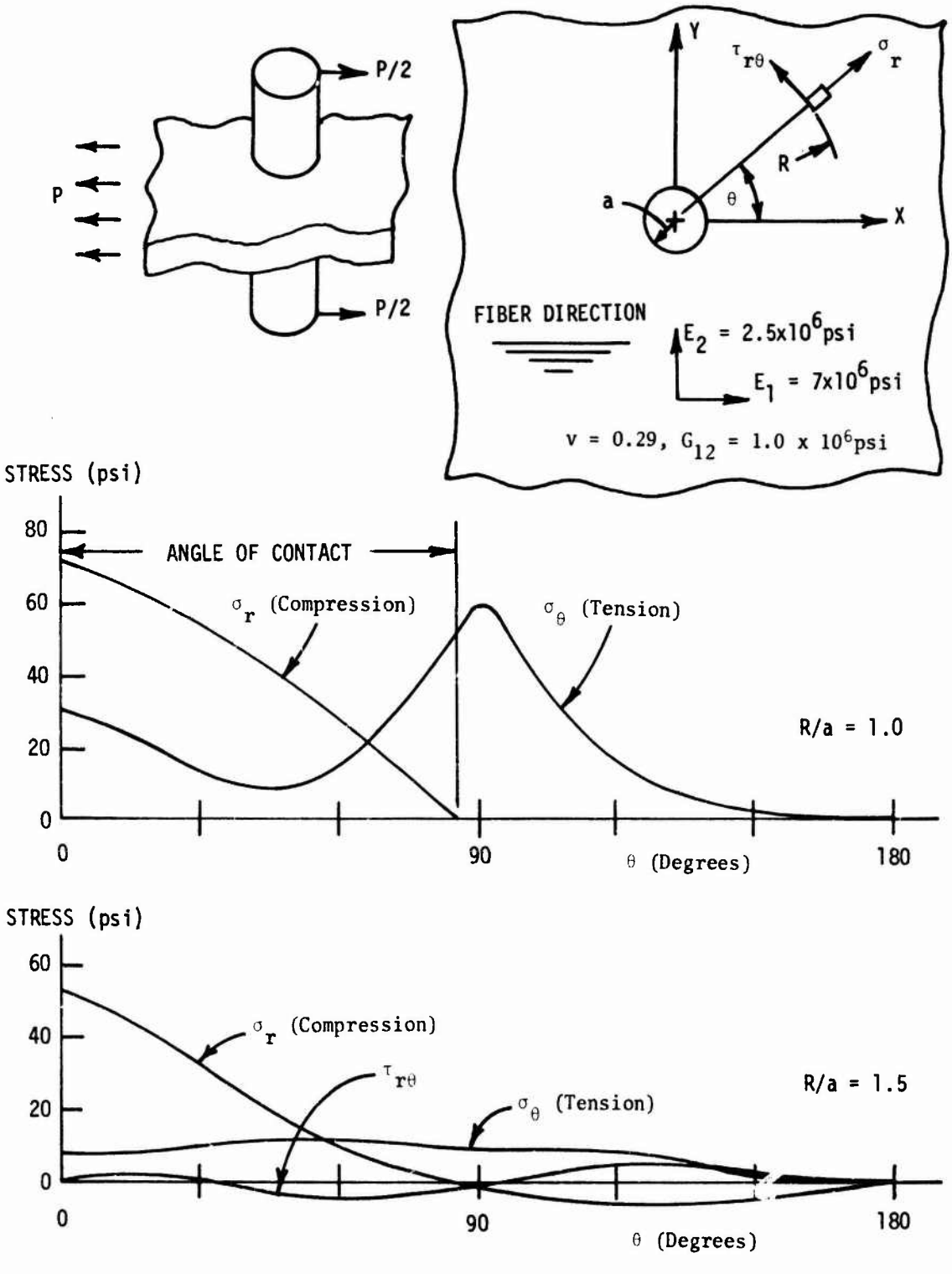

Figure 17. Stress Around Pin Fastener in Orthotropic Plate (P=100 pounds)

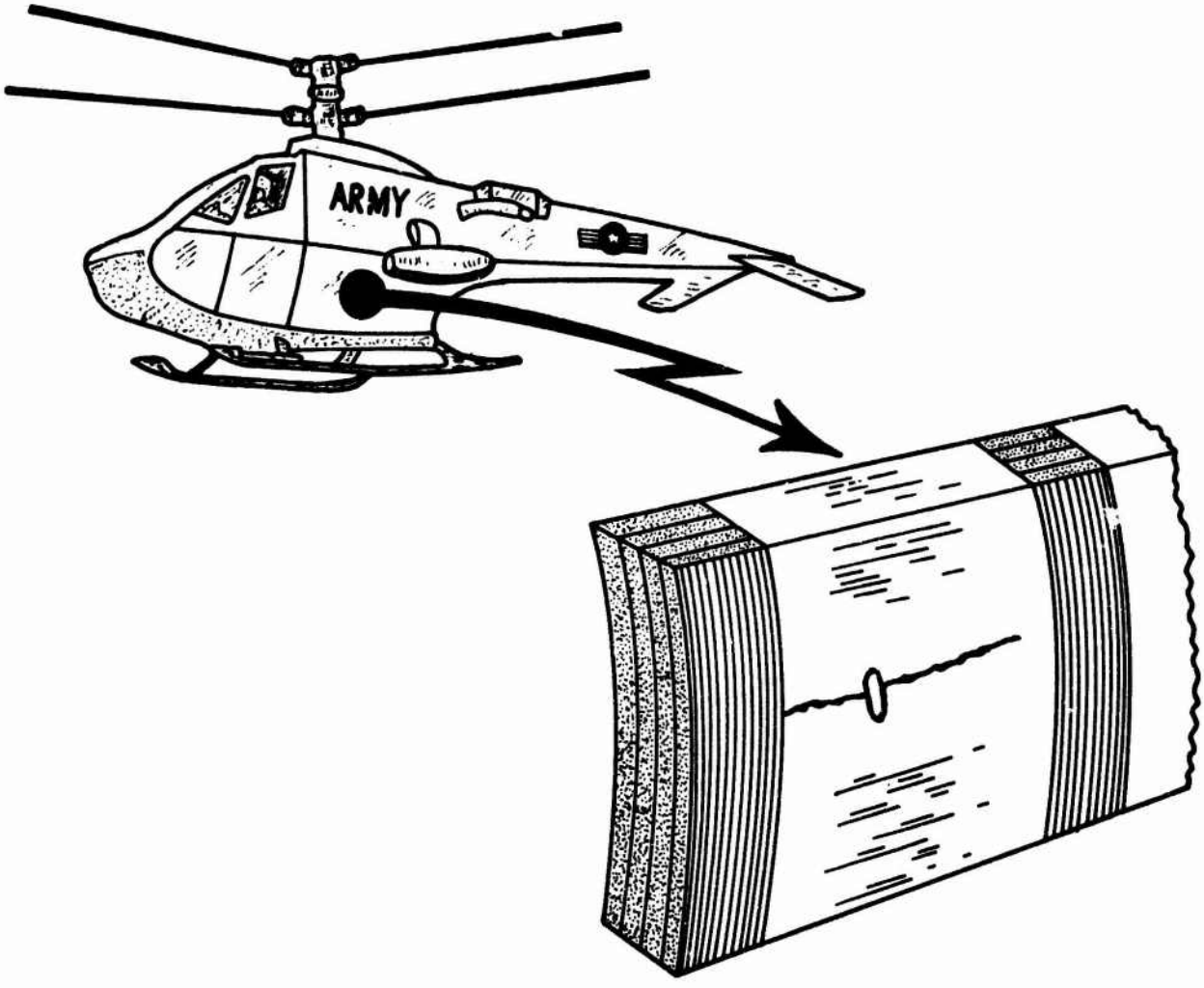

Figure 18. Laminated Strip Concept for Crack Arrest

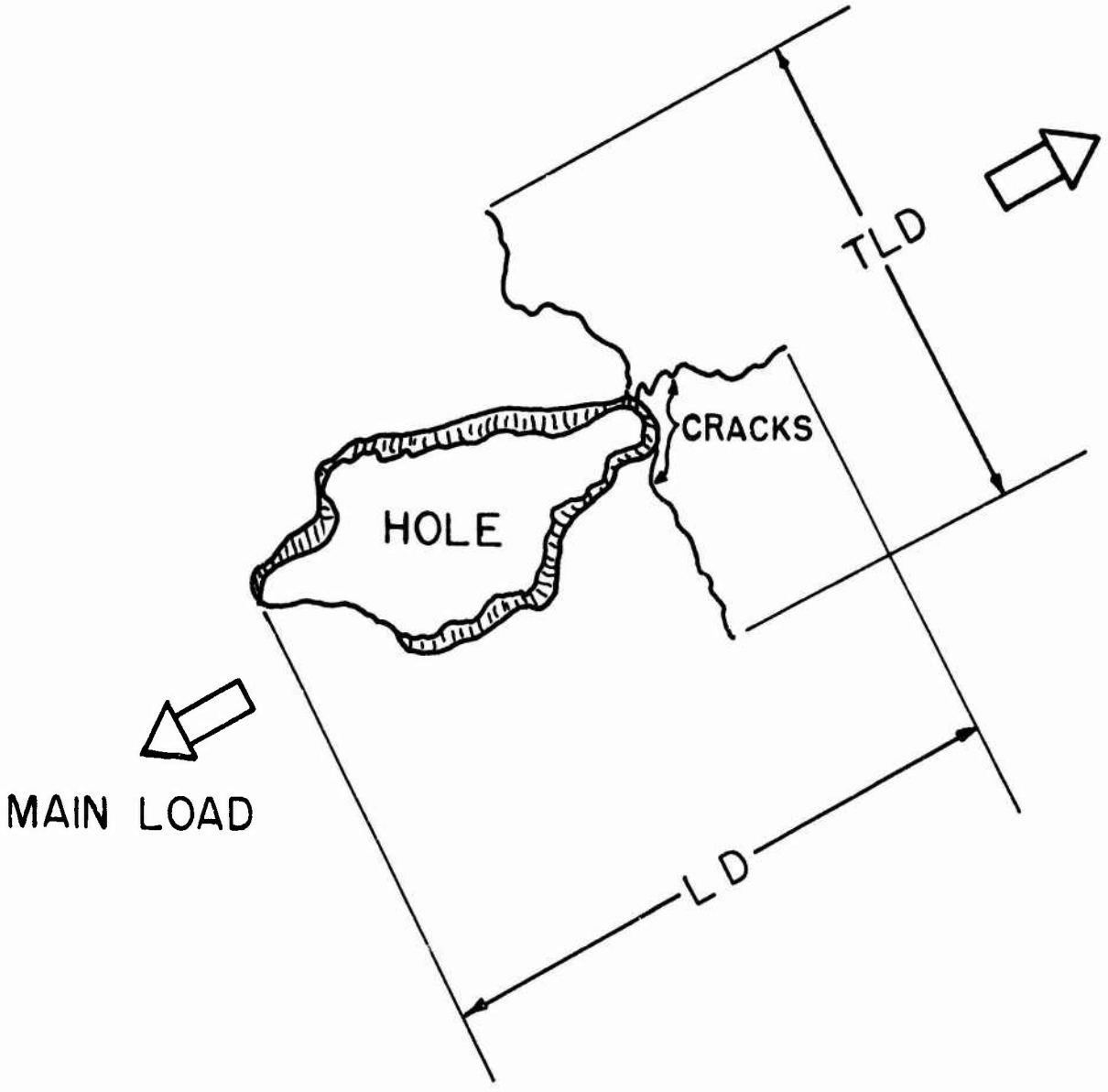

LD: MAXIMUM LATERAL DAMAGE DIMENSION.

TLD: LATERAL DAMAGE DIMENSION TRANSVERSE TO MAIN LOADING DIRECTION.

Figure 19. Illustration Showing Effective Damage "Length"

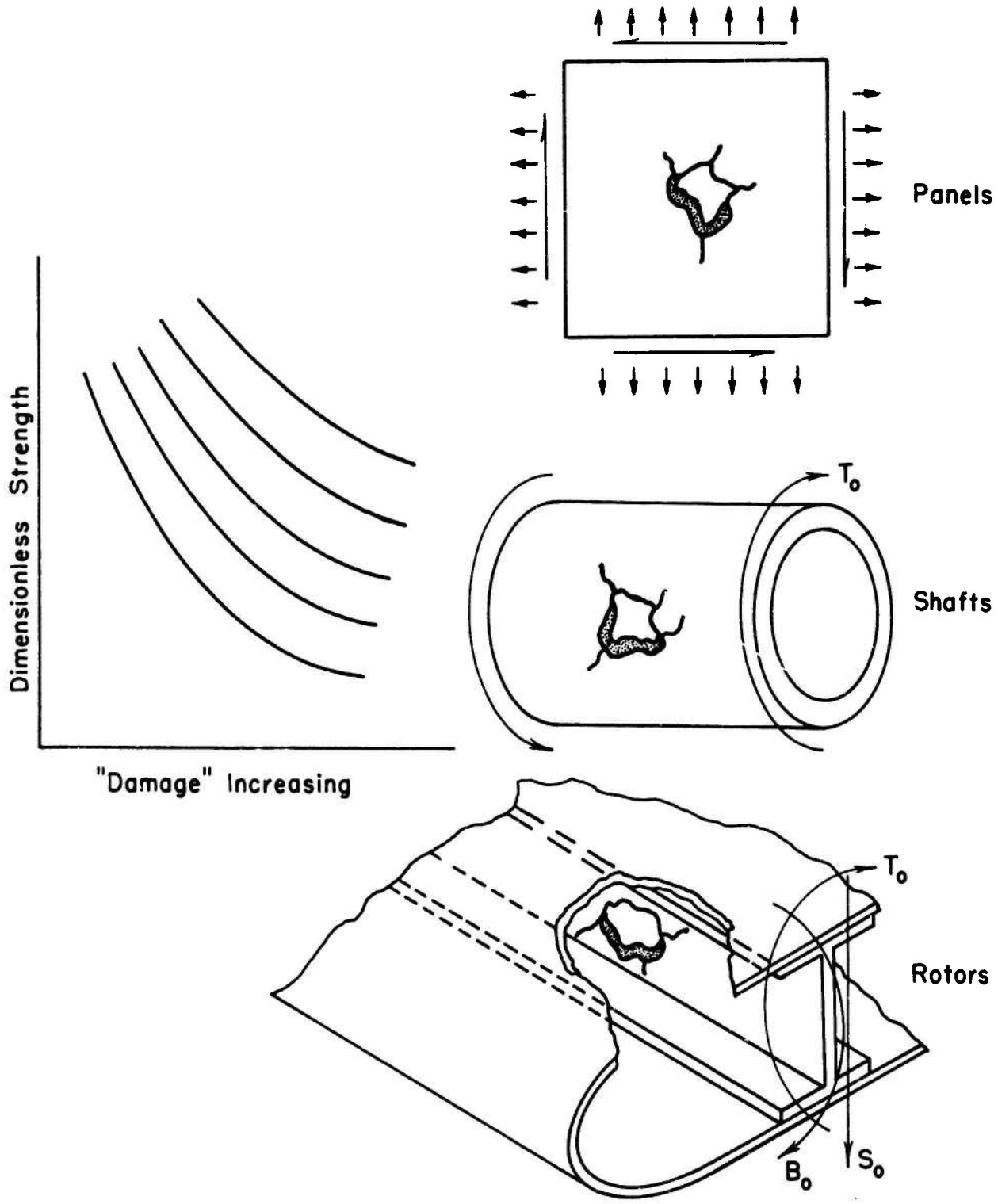

Figure 20. Typical Structural Elements under Consideration in Damage Studies

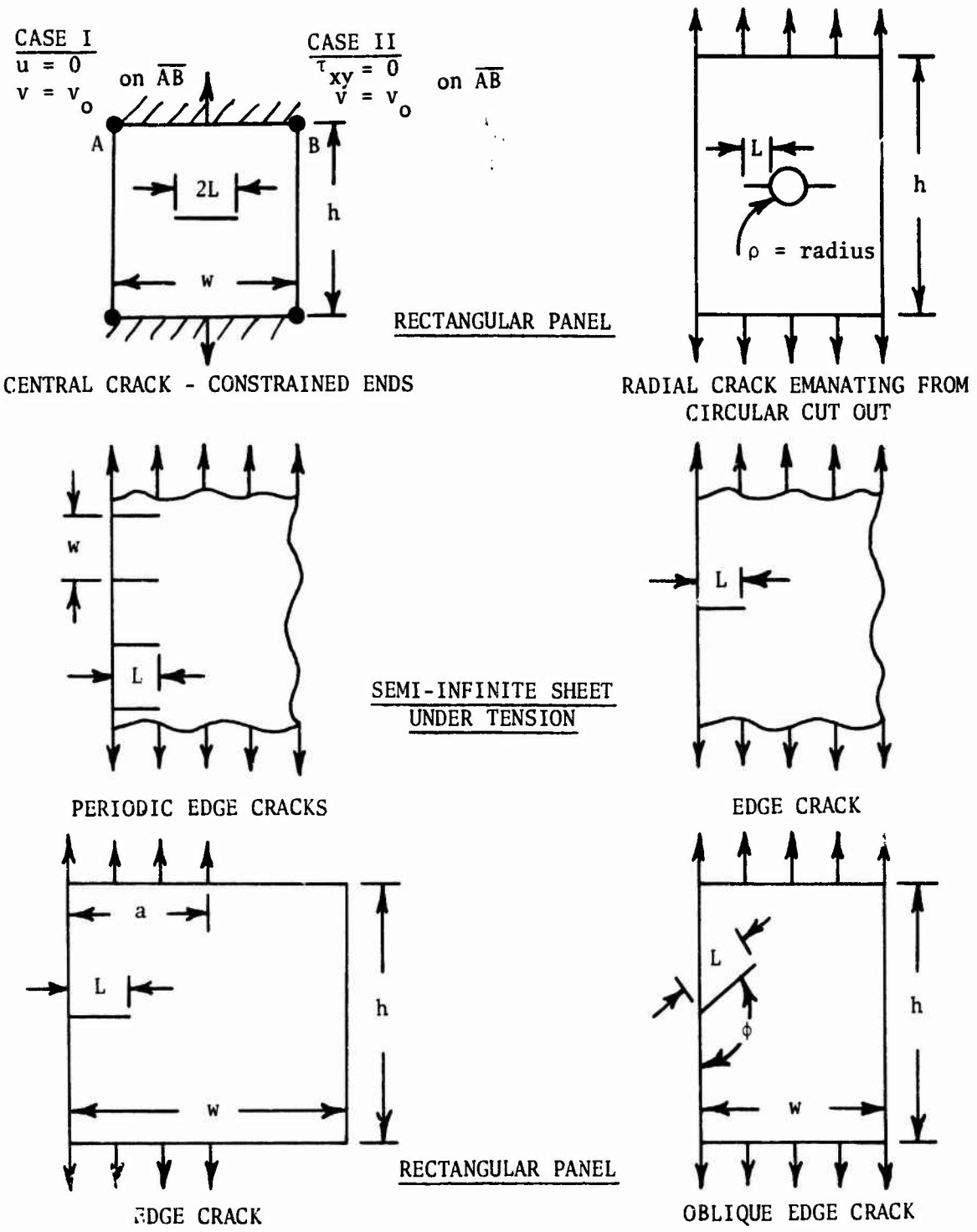

Figure 21. Representative Configurations Treated by Modified Mapping - Collocation Method

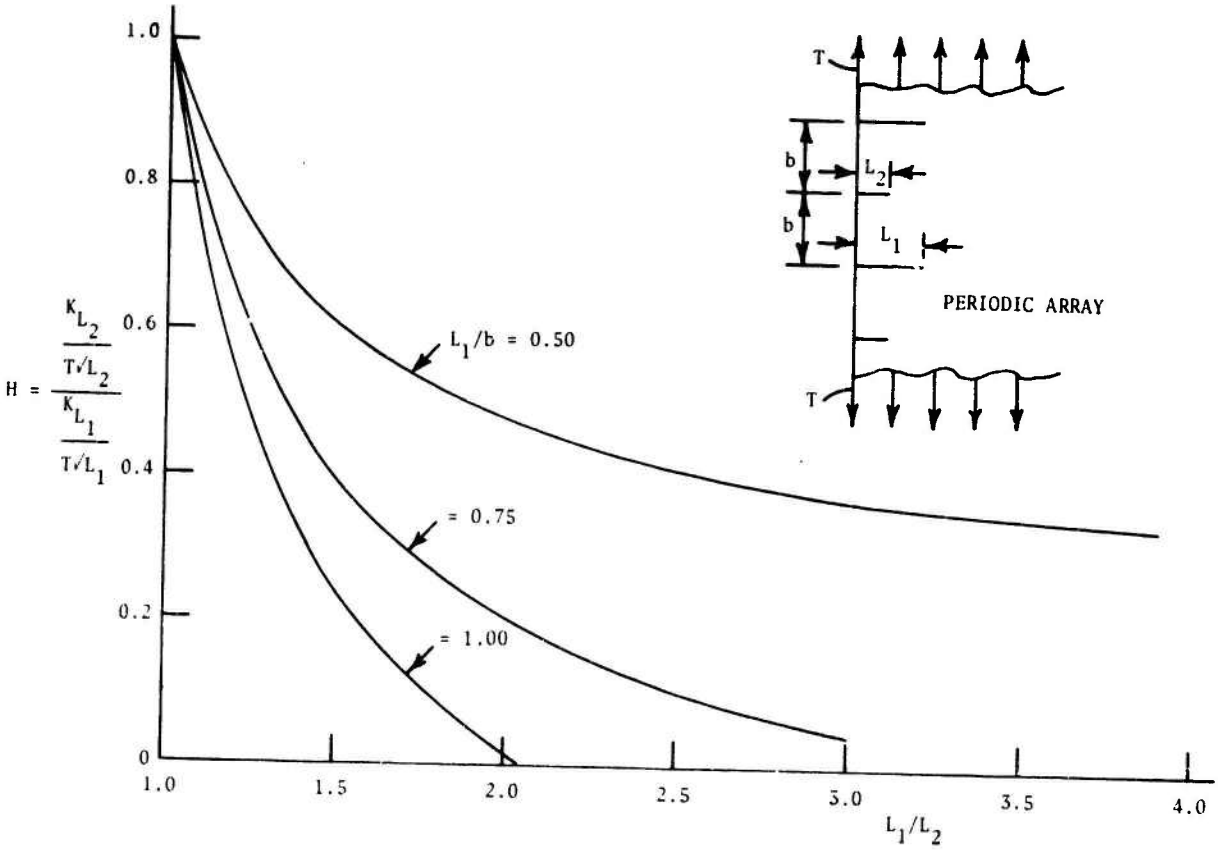

Figure 22. Crack Interaction Effects, in Periodic Array of Cracks

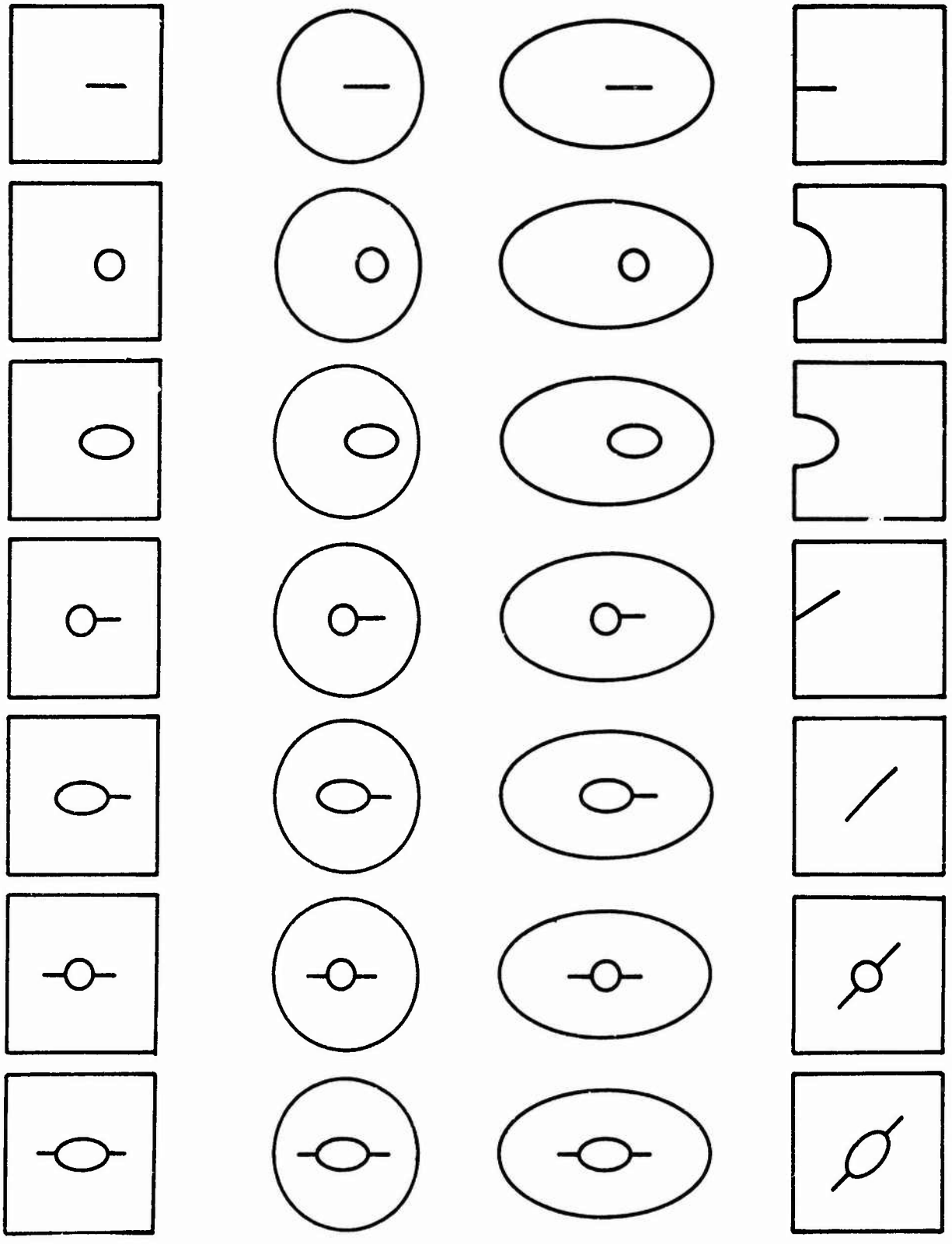

Figure 23. Classes of Problems Tractible by ORTHO

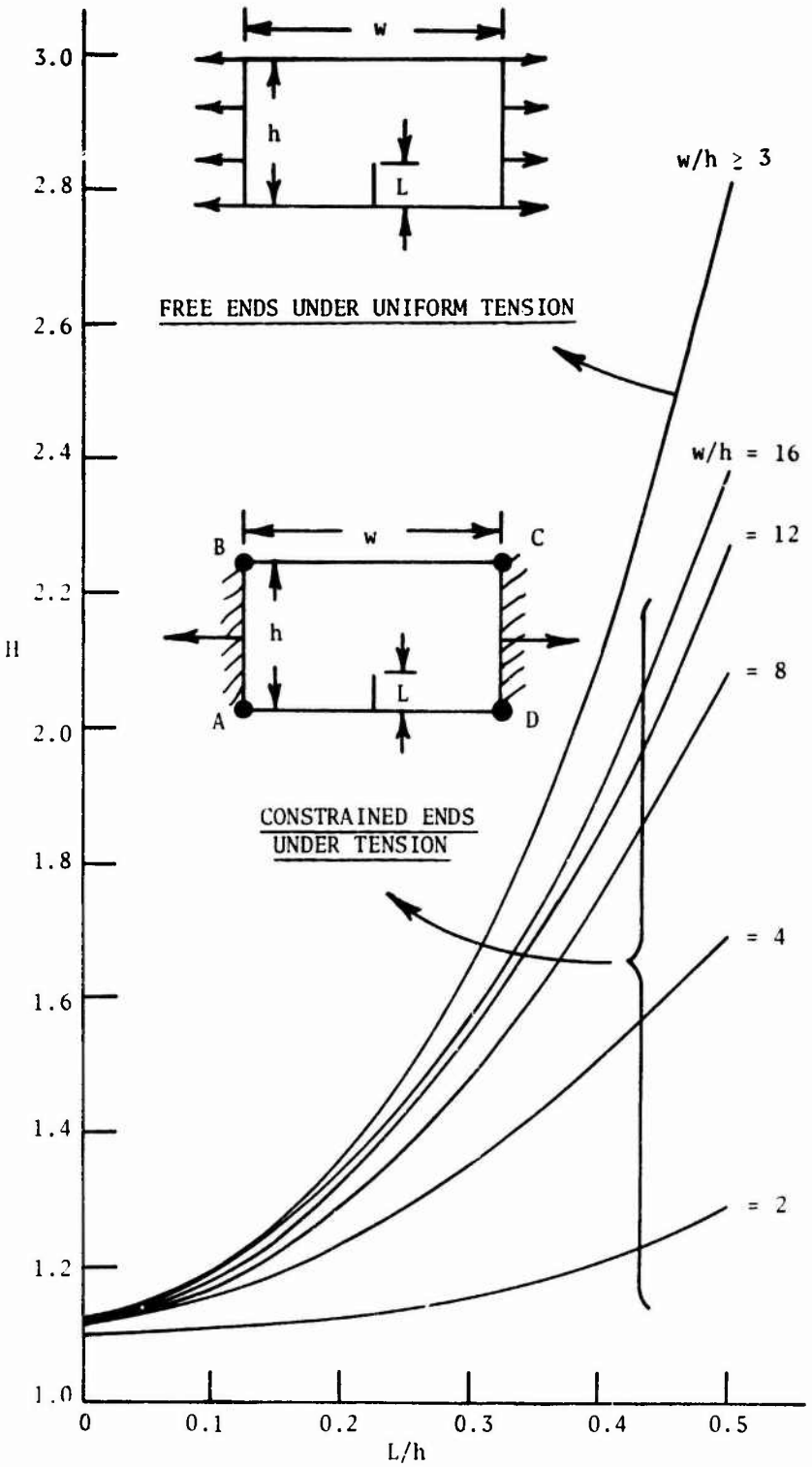

Figure 24. Stress Intensity in Rectangular Panel with Edge Cracks (Typical Results)

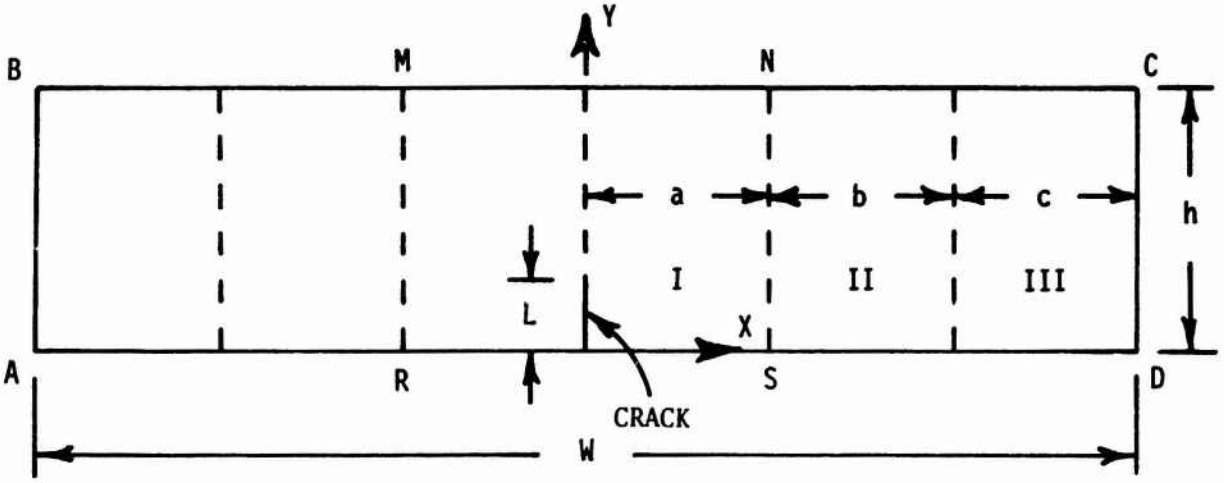

Figure 25. Partitioning Plan (Edge Crack)

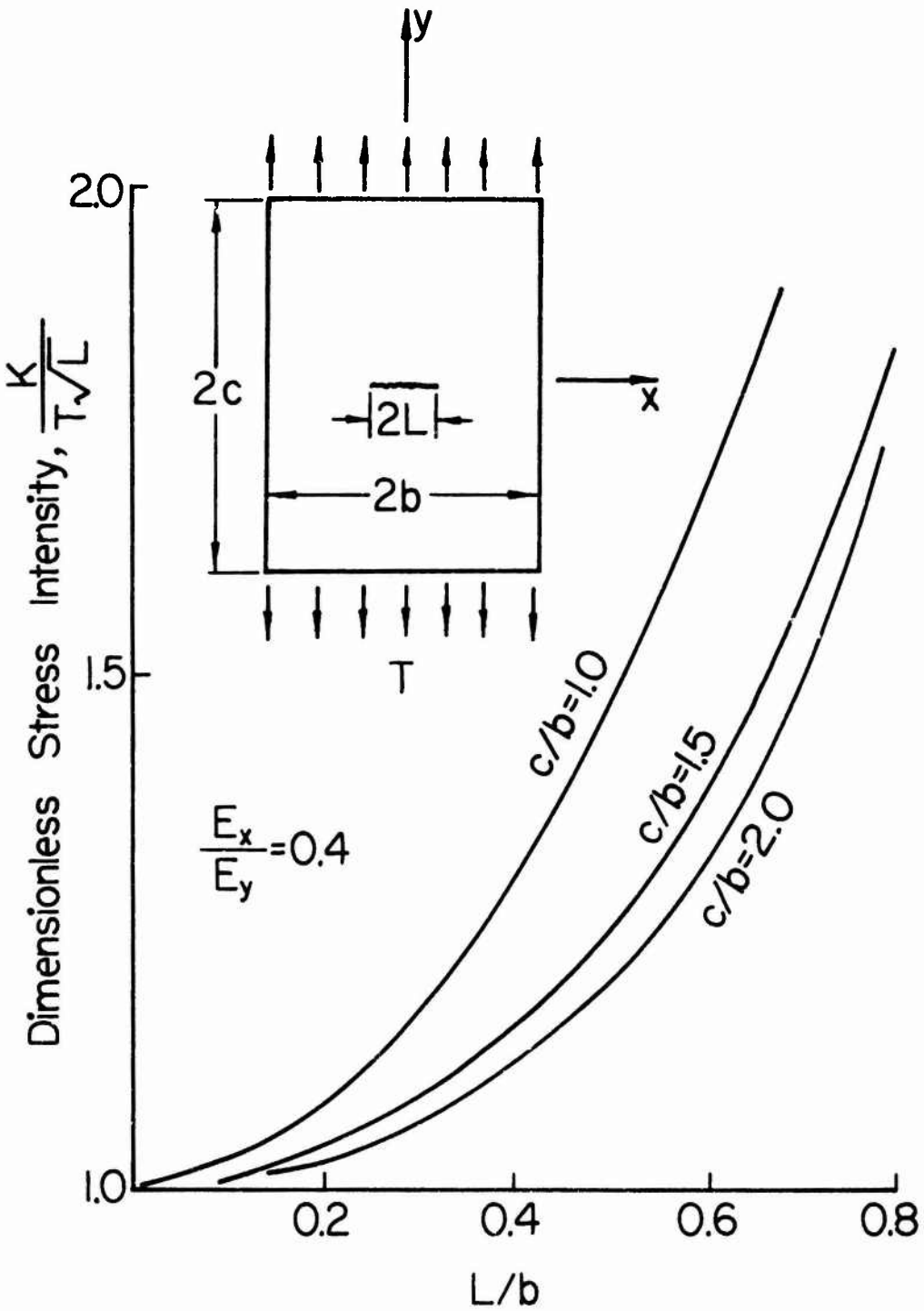

Figure 26. Stress Intensity in Finite Orthotropic Plate

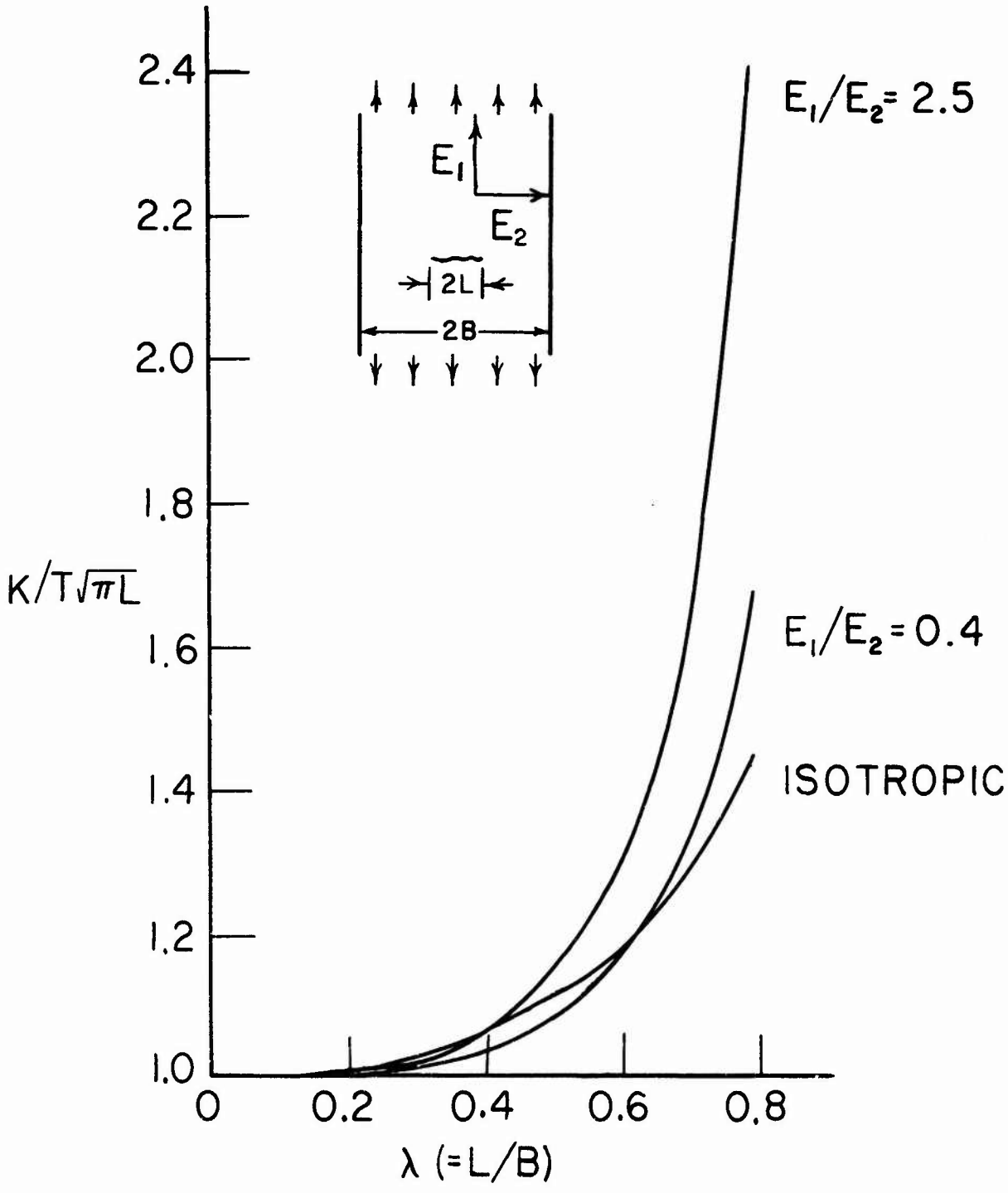

Figure 27. Effect of Orthotropic Parameters on Normalized Stress Intensity Factor in Infinite Strip

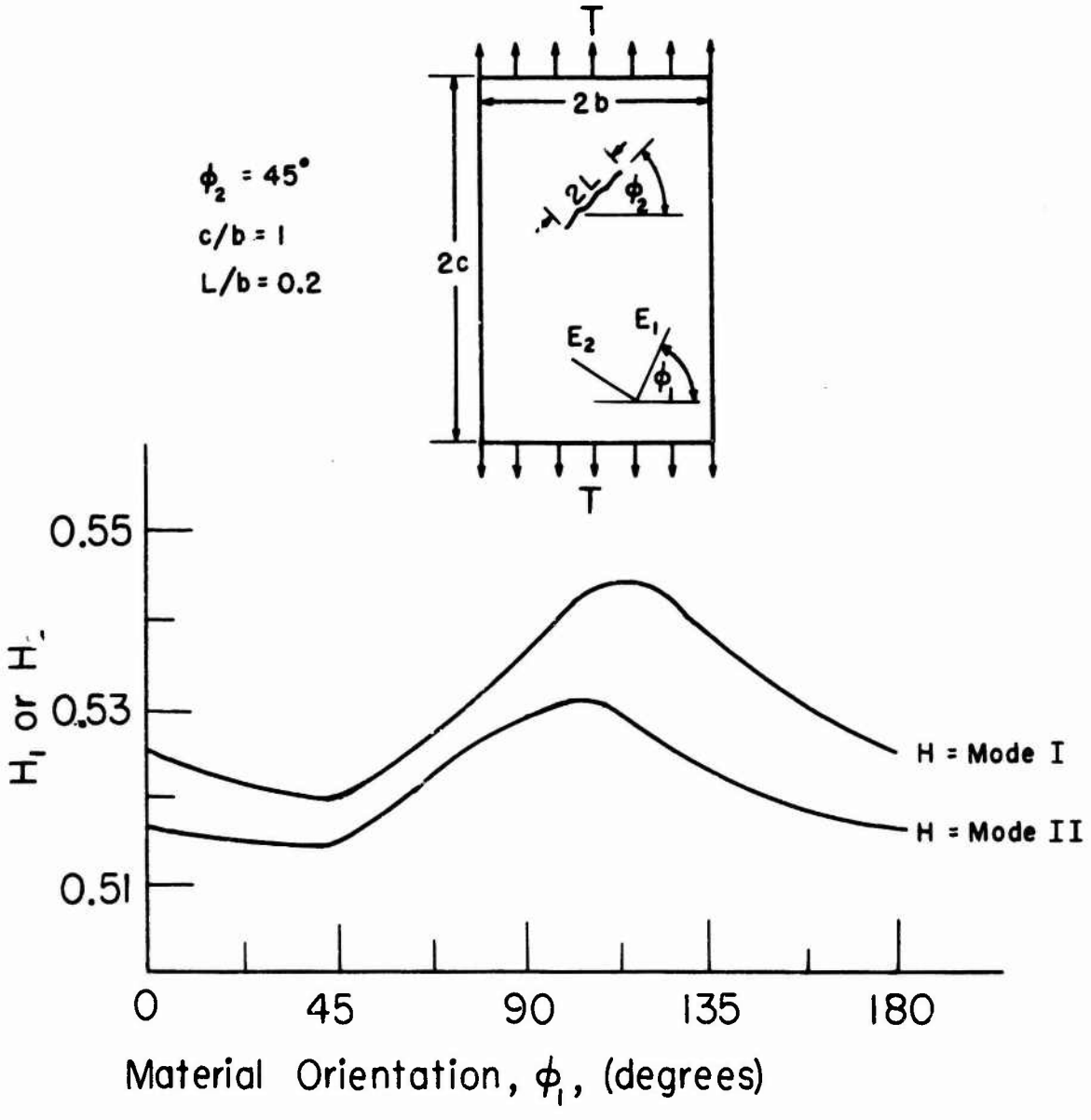

Figure 28. Variation of Normalized Stress Intensity Factor with Material Orientation Angle ϕ_1

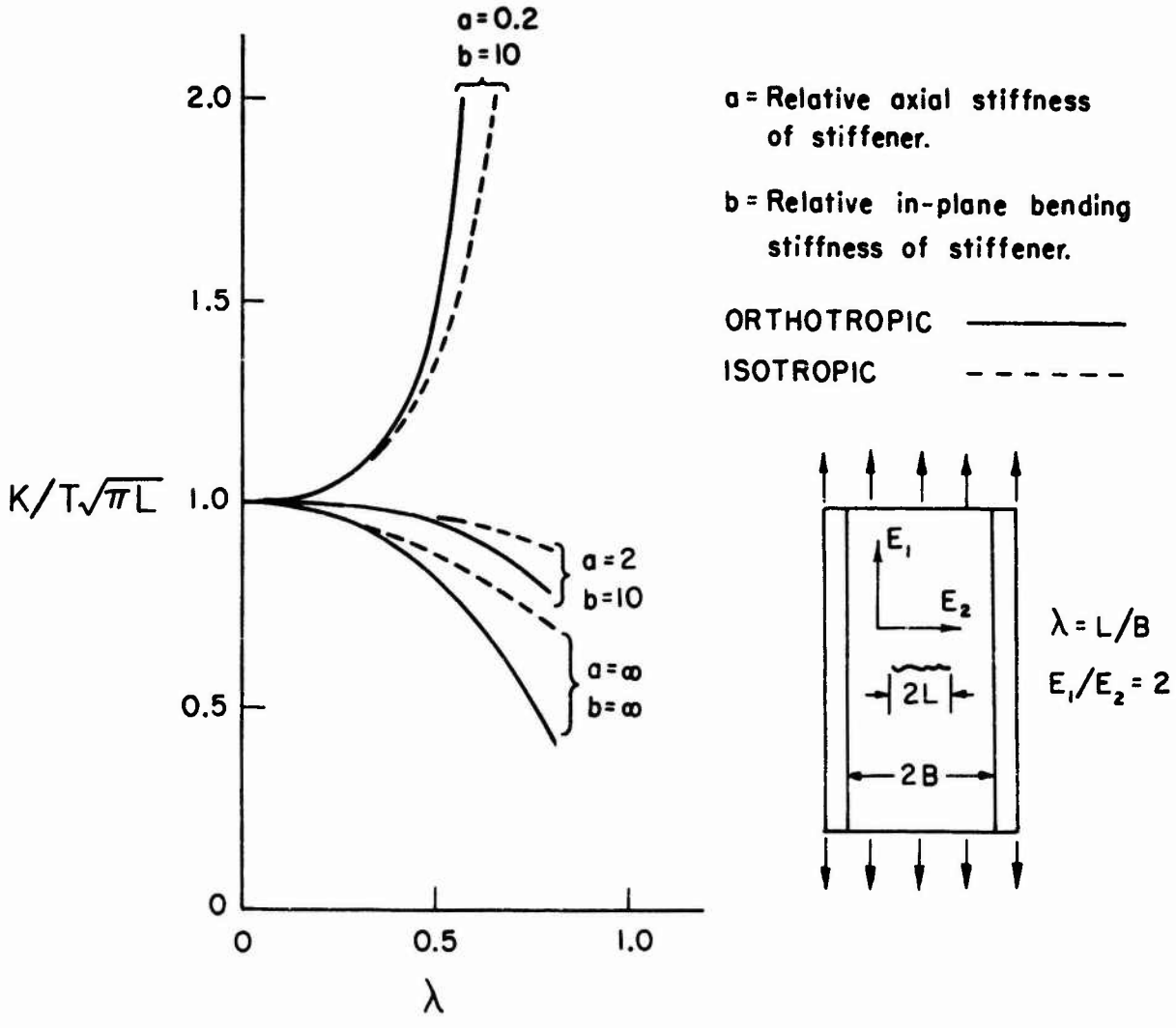

Figure 29. Effect of Stiffener Flexibility on Normalized Stress Intensity Factor

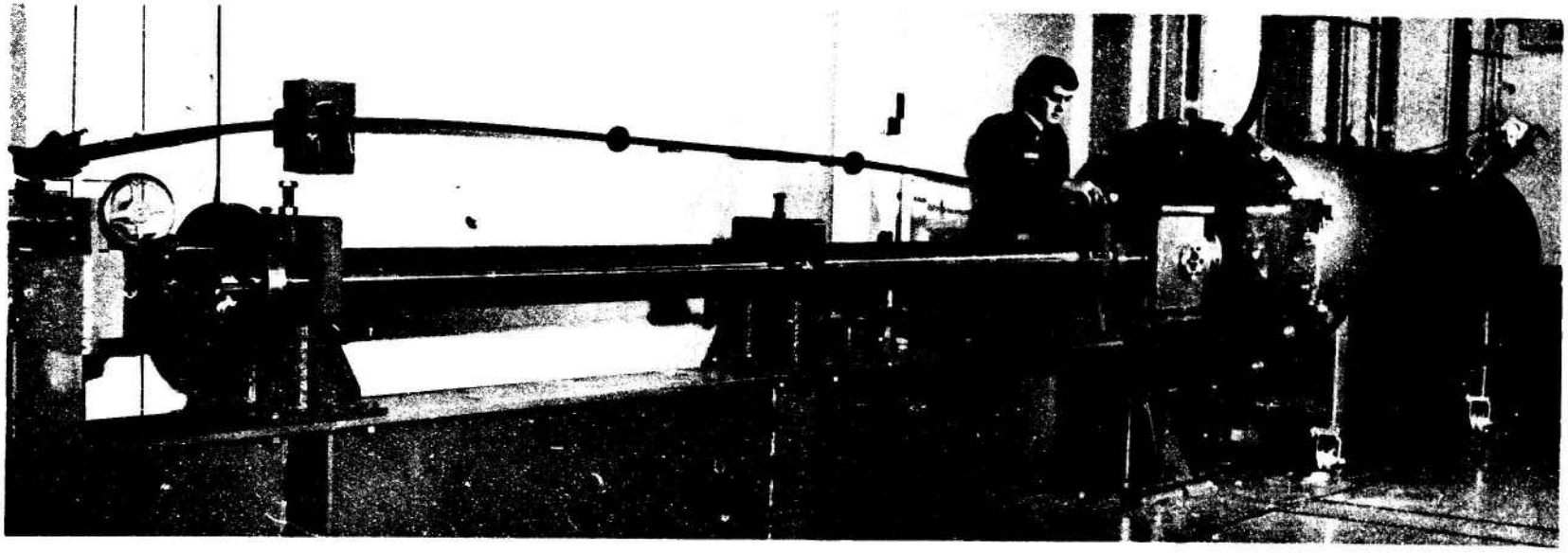

Figure 30. Photograph of 4-inch Plate Accelerator Facility

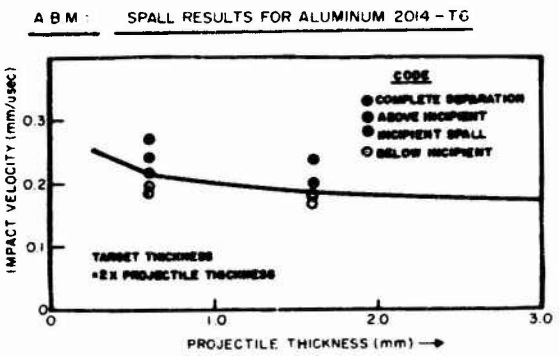

PLATE ACCELERATOR: - A continuous range of velocities (from 100 to 4000 ft/sec) is achievable by adjusting the gas pressure in the breech. (Breech volume is 1 cu ft and maximum pressure is 6000 psi) For the highest velocities the projectile weight is about one pound with the 4-inch internal diameter launch tube. The impact stress range is as follows:

PROJECTILE	TARGET MATERIALS (in kb)			
Material	Al	Steel	W	Plexiglas
Aluminum	110	155	190	45
Steel	155	270	370	55
Tungsten	190	370	570	65
Plexiglas	45	55	65	25

1 Kilobar = 14,504 psi

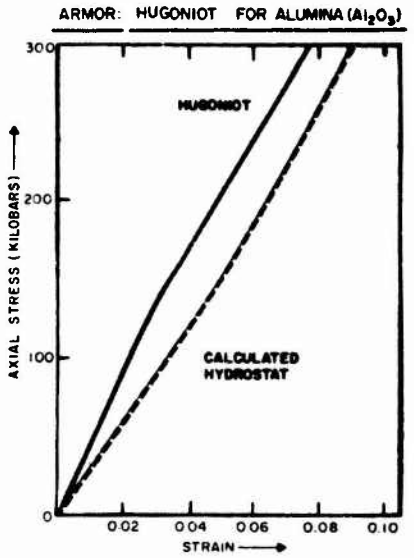

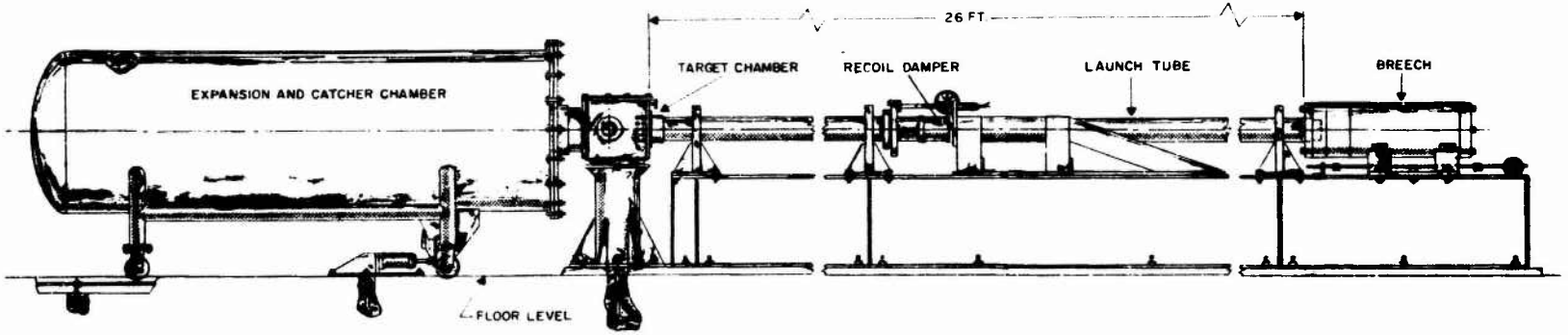

Figure 31. Schematic of 4-inch Plate Accelerator Facility

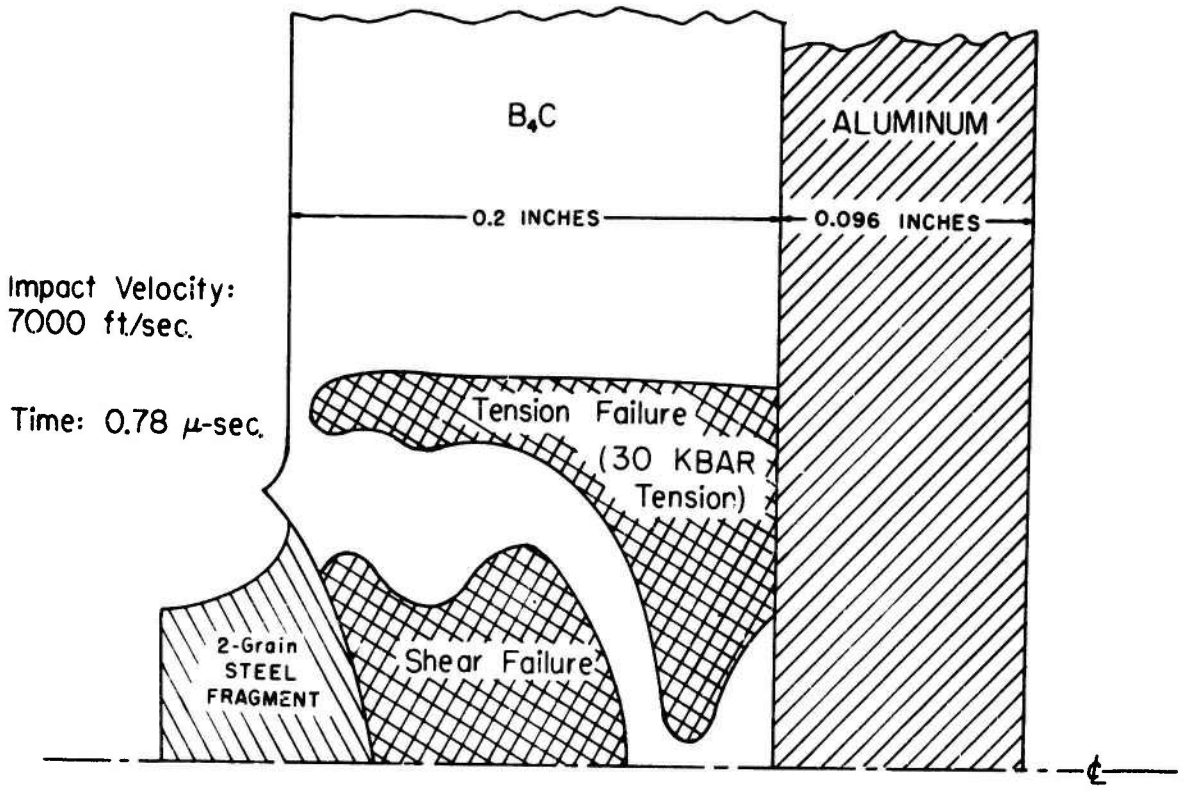

Figure 32. Computer Simulation of Penetration in Composite Armor System

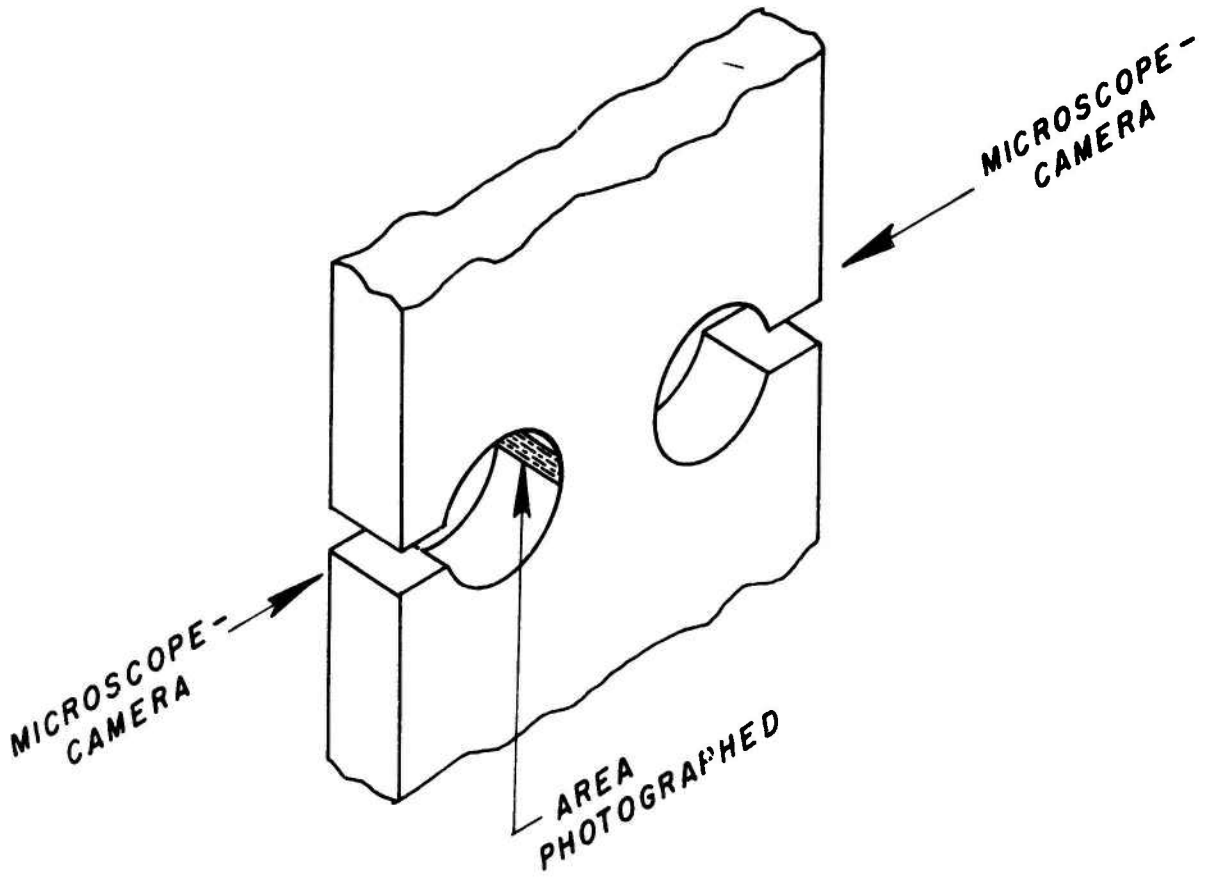

Figure 33. Schematic View of Notched Region of Specimen

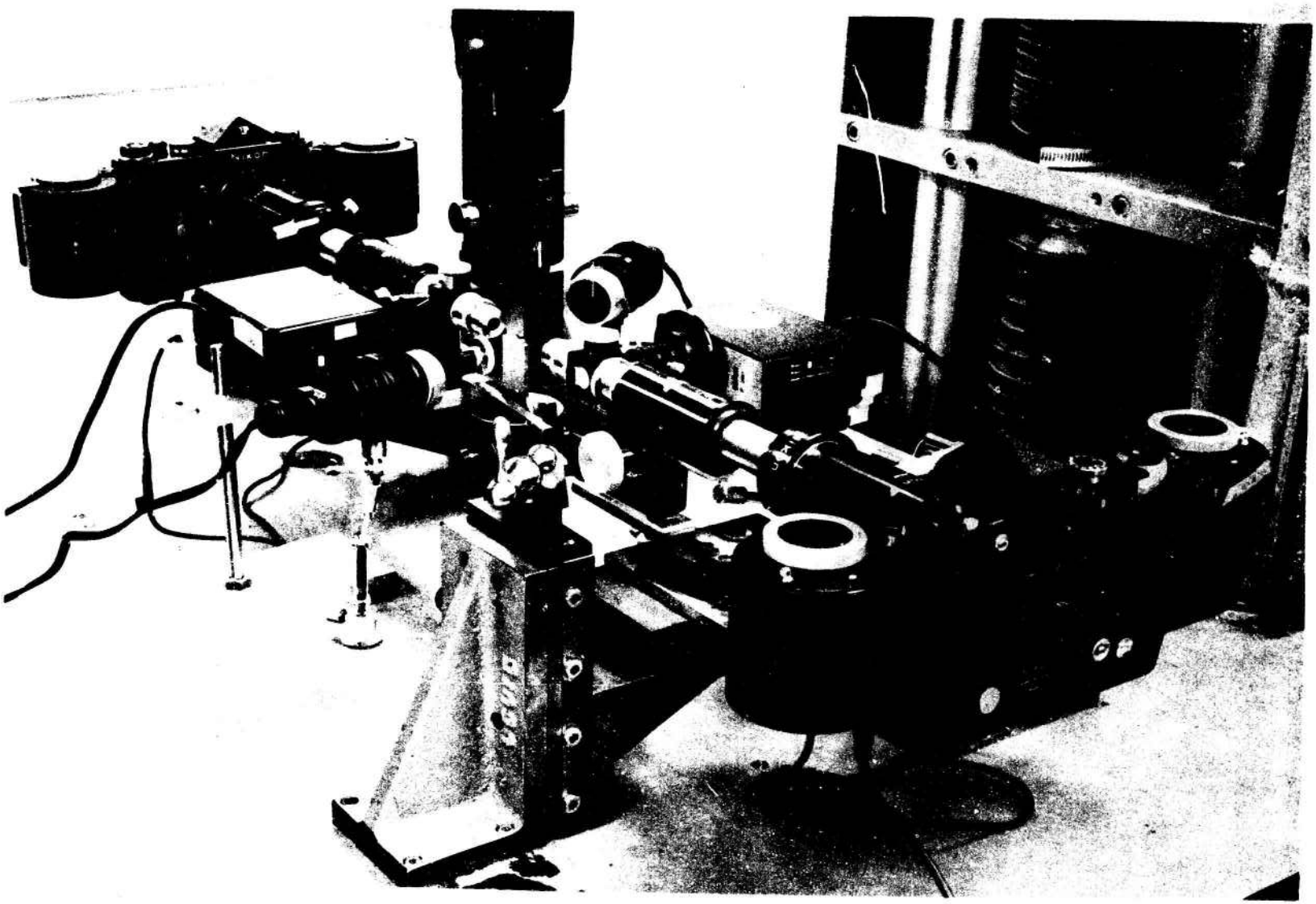

19-066-632/AMC-71

Figure 34. Setup for Photomicrographic Recording of Crack Initiation

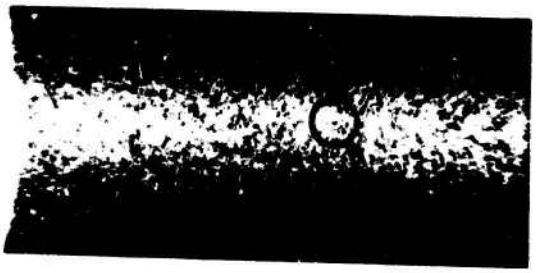

5200 CYCLES

7300 CYCLES

5400 CYCLES

9300 CYCLES

5700 CYCLES

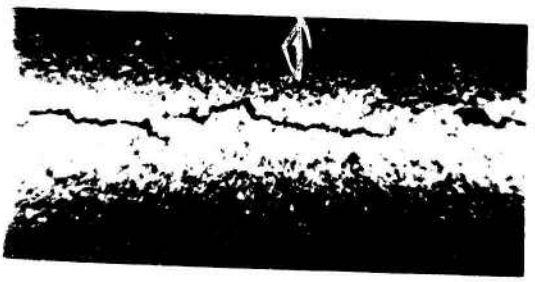

11728 CYCLES

19-066-517/AMC-72

Figure 35. Crack Initiation Progression

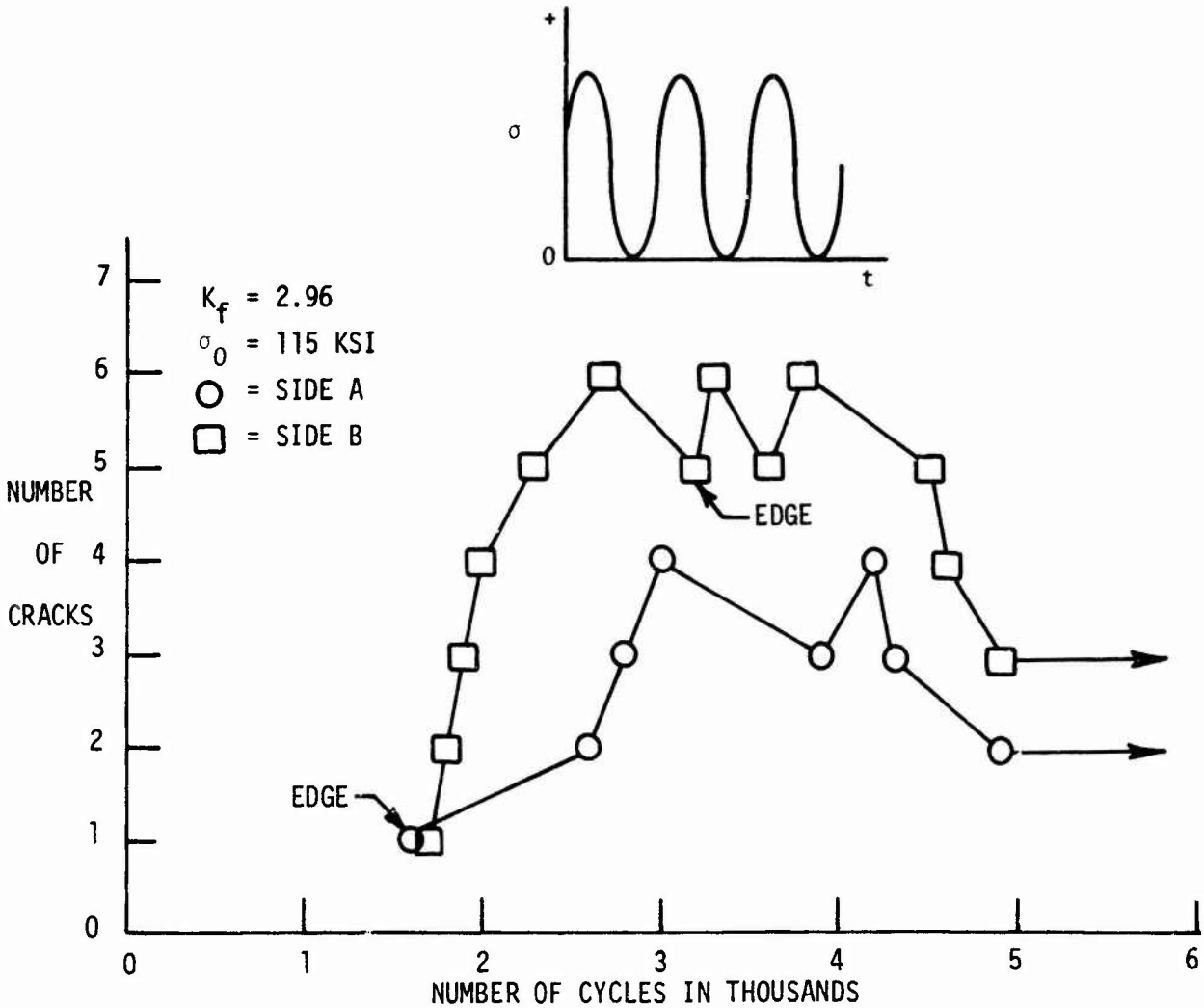

Figure 36. Crack Count as a Function of Loading Cycles

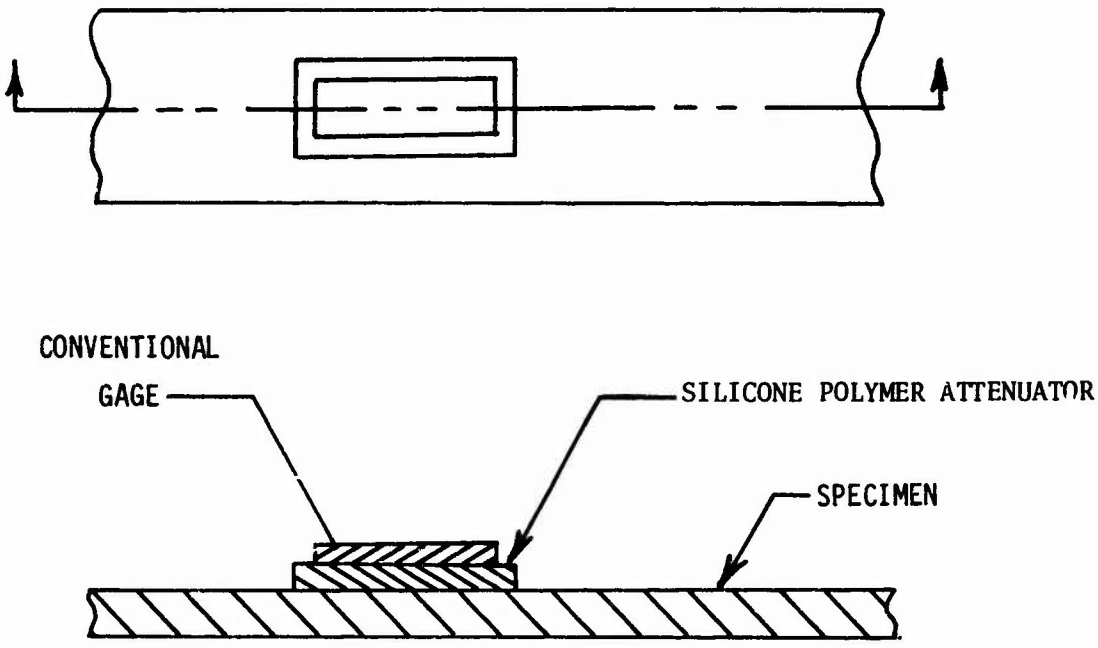

Figure 37. Strain Gage/Pad Configuration

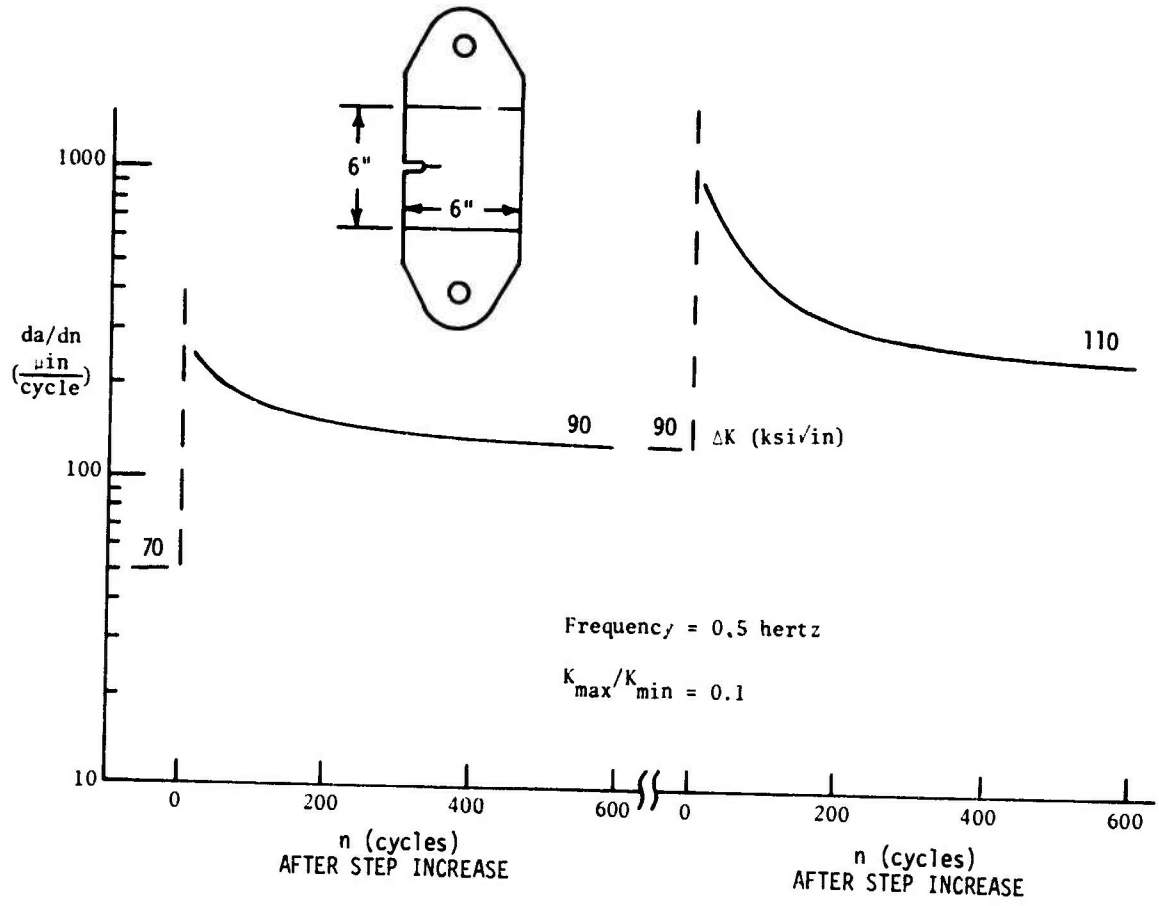

Figure 38. Transient Crack Growth Behavior after Step Change in Loading

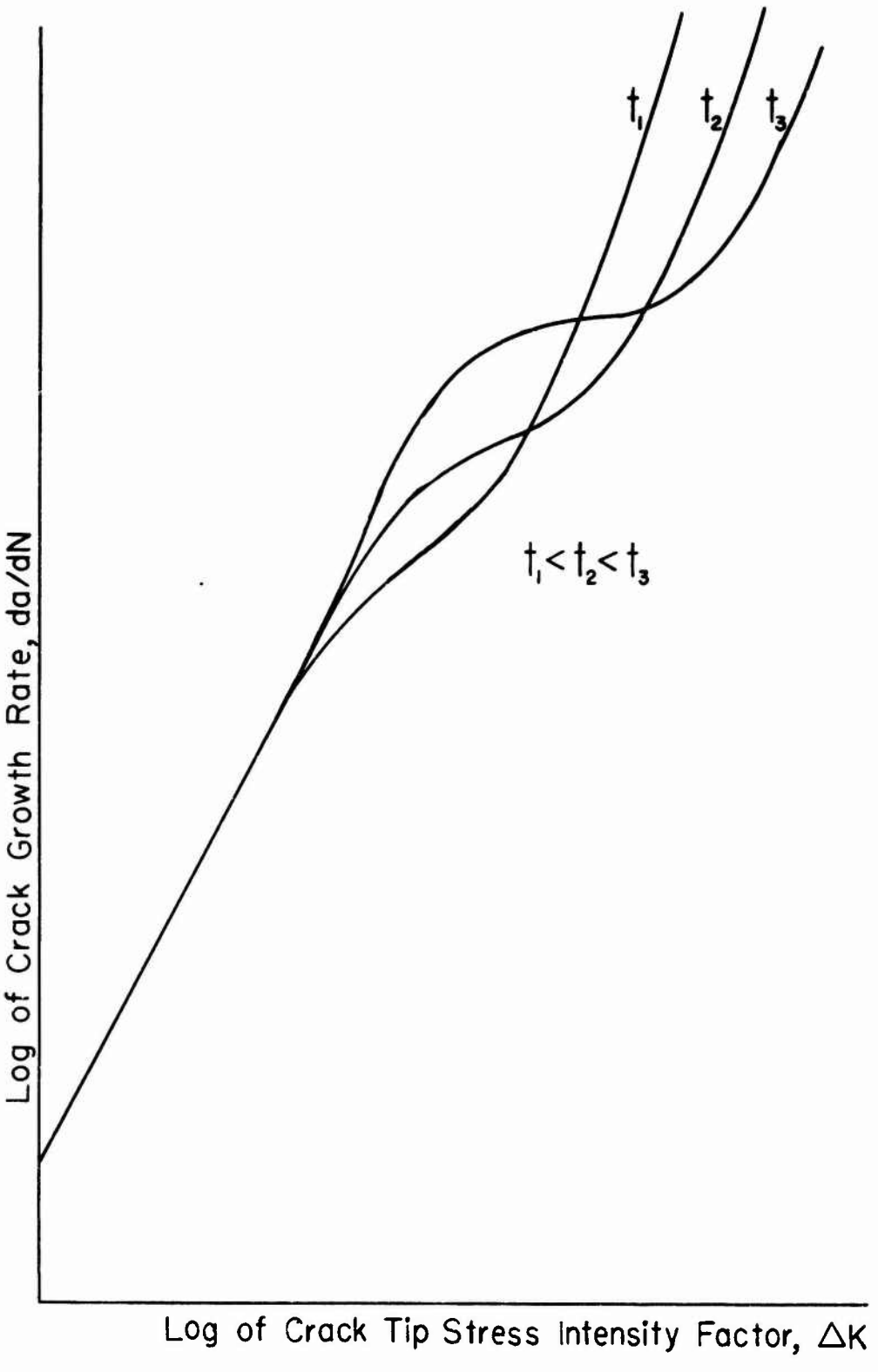

Figure 39. Predicted Thickness Effect on Crack Growth Rates

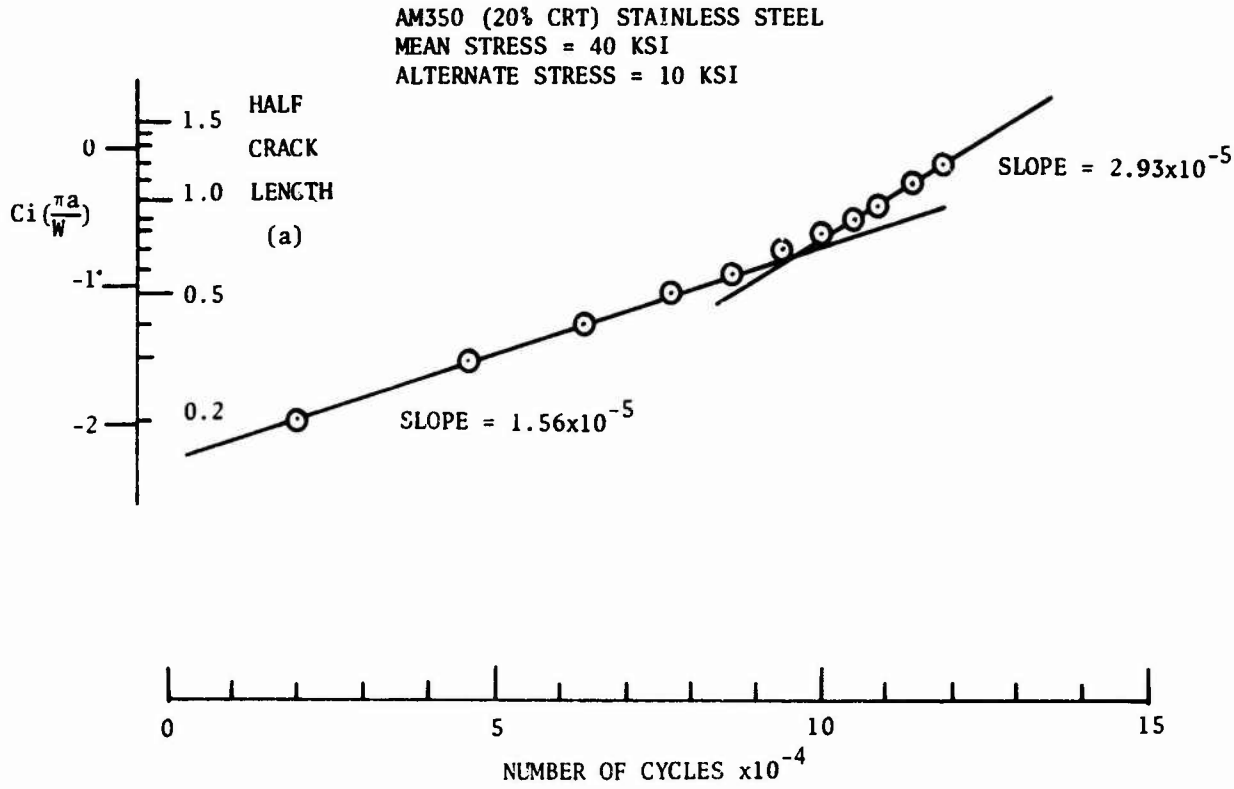

Figure 40. Typically Observed Crack Length versus Number of Cycles

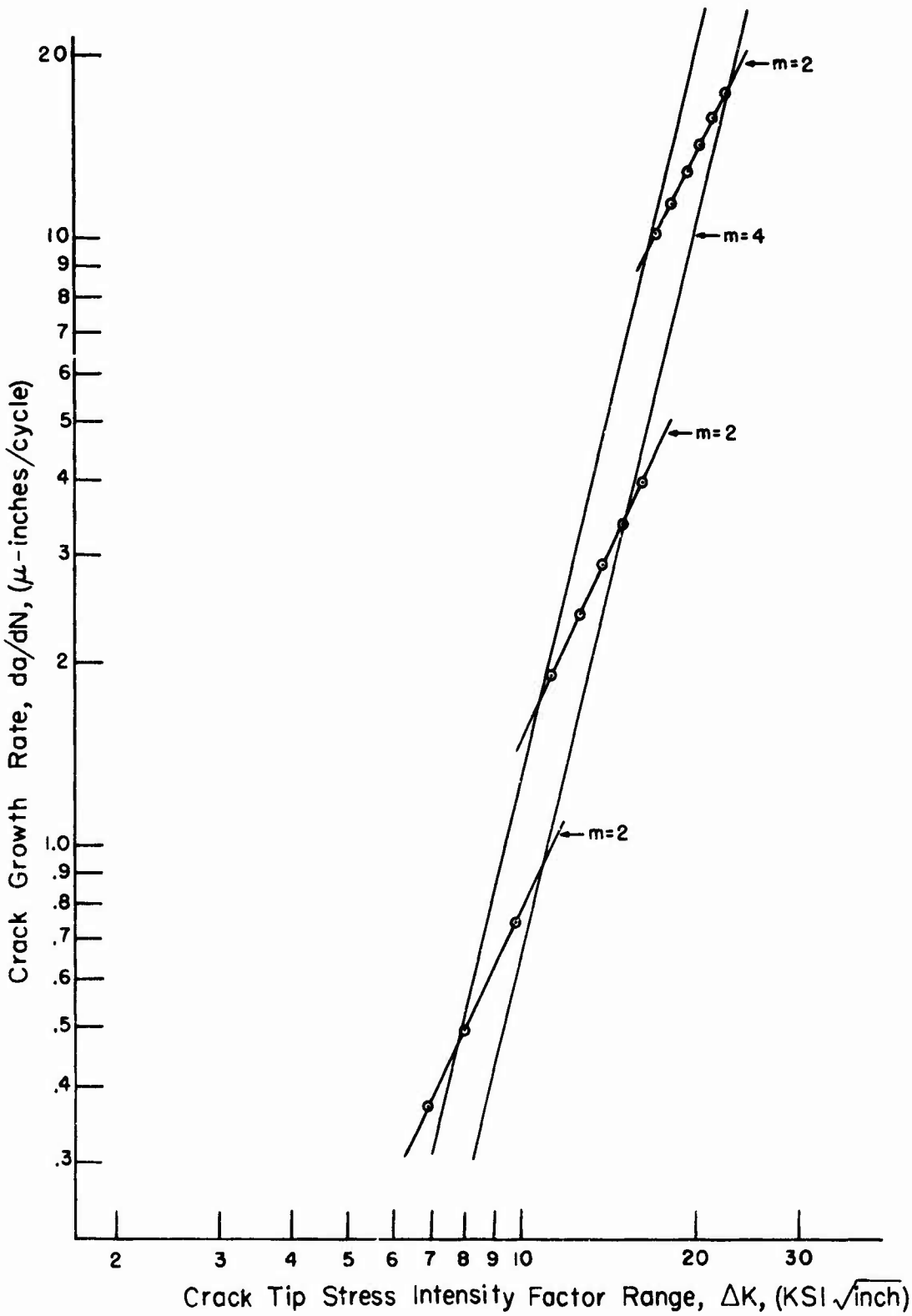

Figure 41. Discontinuous Crack Growth Rate as Function of Stress Intensity Factor

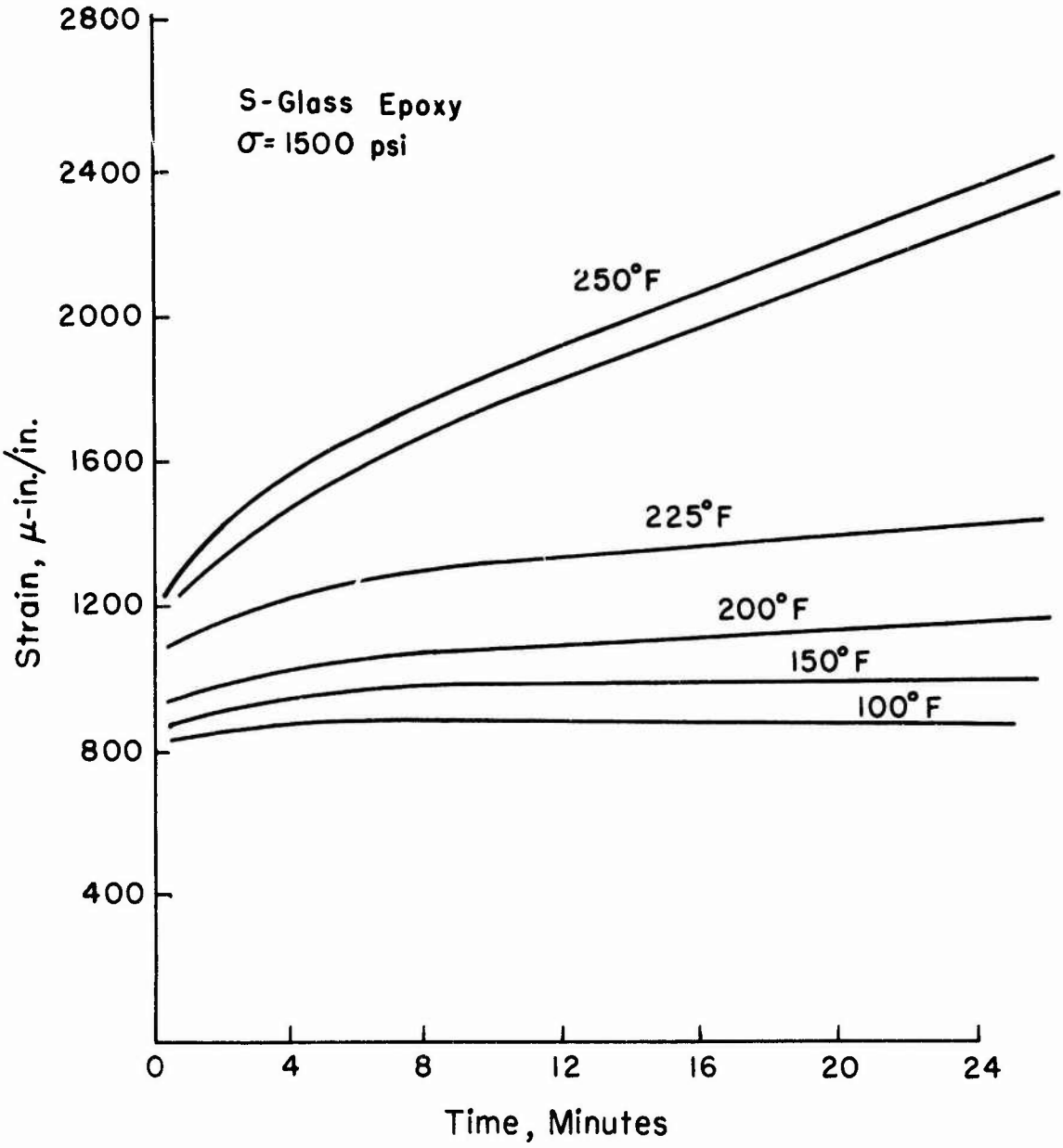

Figure 42. Creep Data for S-Glass/Epoxy

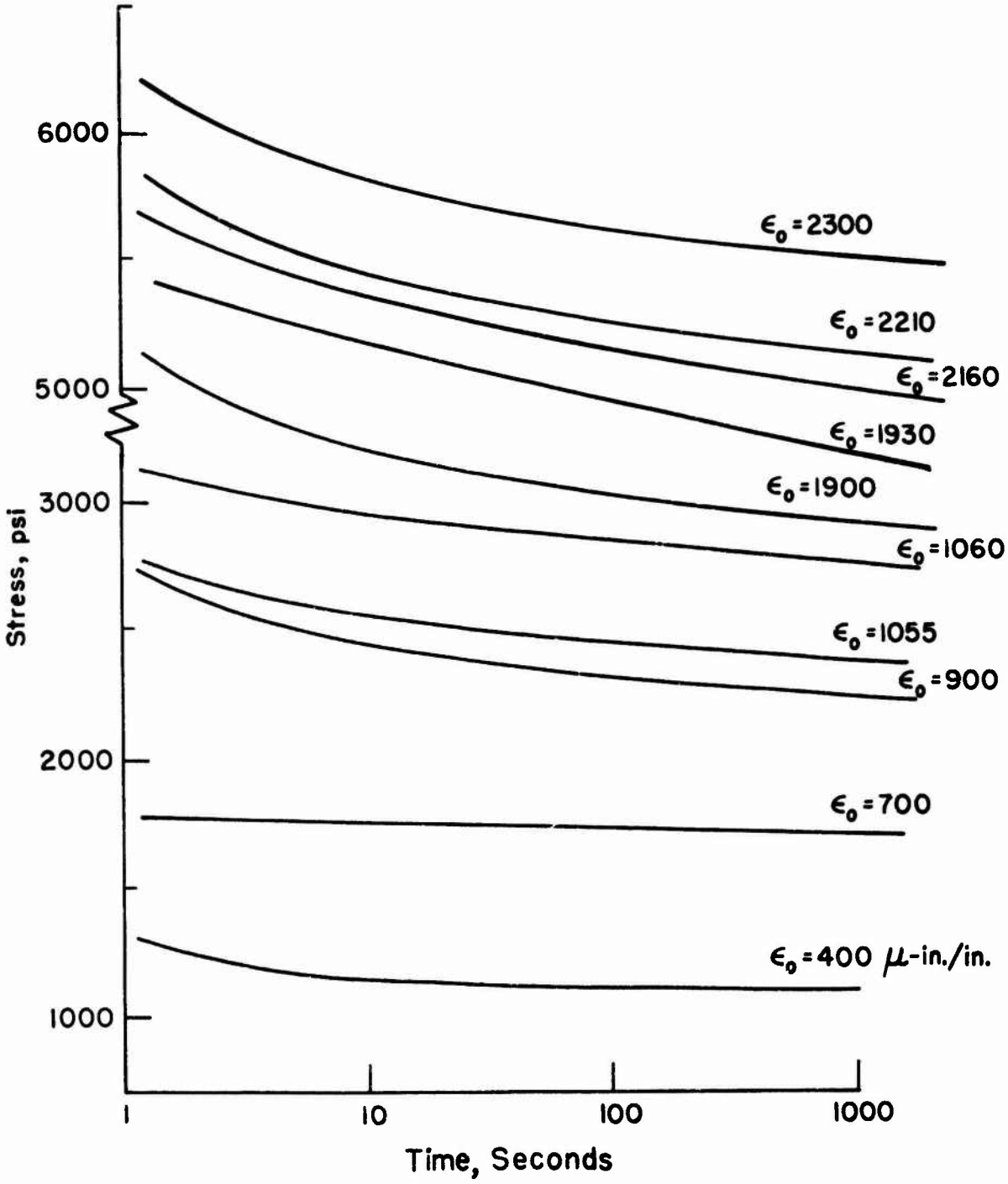

Figure 43. Relaxation Data for Boron/Epoxy at 73 F

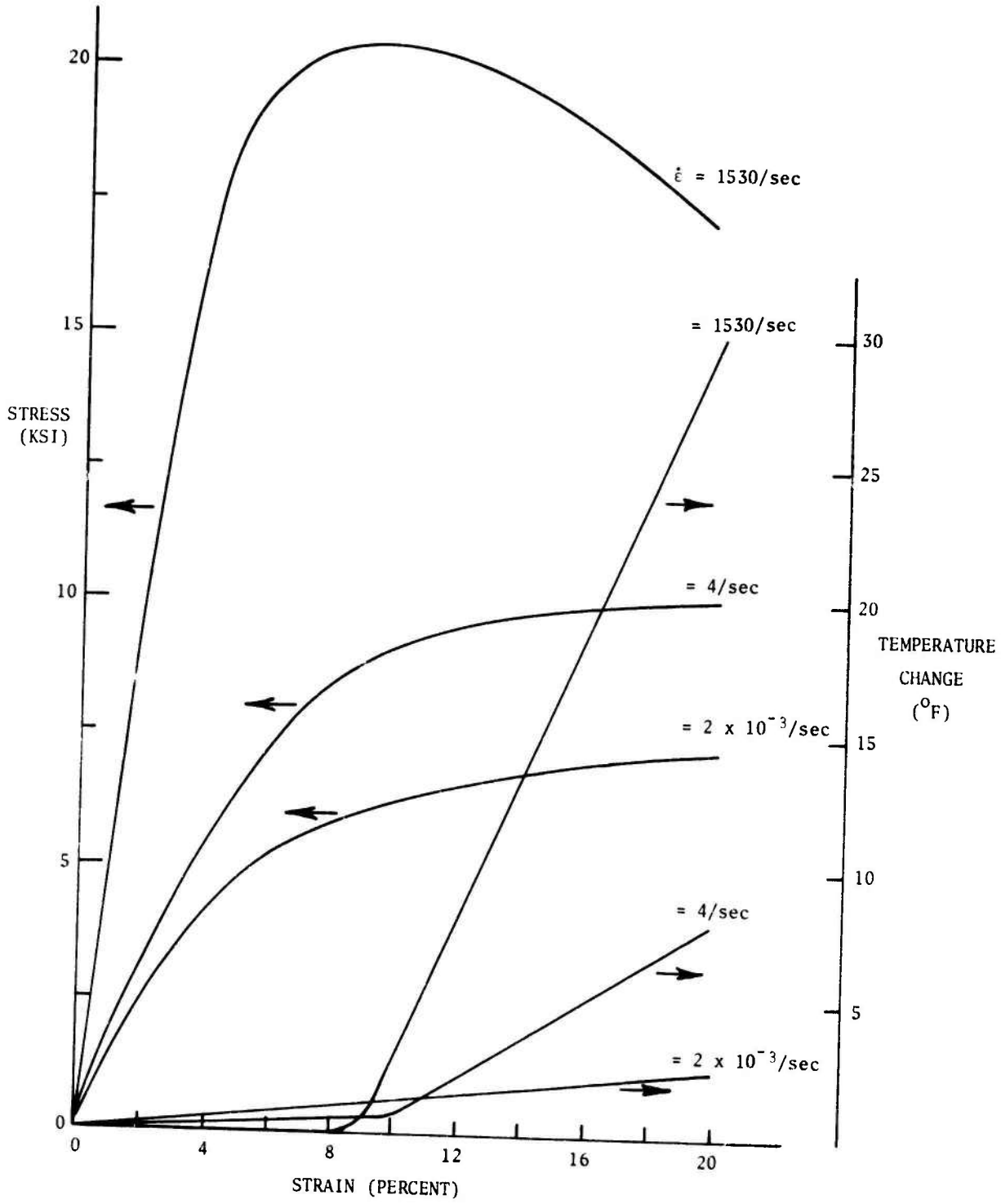

Figure 44. Dynamic Constitutive Relations for Polypropylene